Electronic Supplementary Material (ESI) for Chemical Communications.

Electronic supplementary information

Linear assembly of porphyrin–C_{60} complex confined in vertical nanocylinders of amphiphilic block copolymer films

Takuya Kamimura,[a] Motonori Komura,*[b] Hideaki Komiyama,[c] Tomokazu Iyoda[c] and Fumito Tani*[a]

[a] *Institute for Materials Chemistry and Engineering, Kyushu University, 6-10-1 Hakozaki, Higashi-ku, Fukuoka, Fukuoka 812-8581, Japan.*

E-mail: tanif@ms.ifoc.kyushu-u.ac.jp; Fax: +81-92-642-2732; Tel: +81-92-642-2732

[b] *National Institute of Technology, Numazu College, 3600 Ooka Numazu, Shizuoka 410-8501, Japan.*

E-mail: m-komura@numazu-ct.ac.jp; Fax: +81-55-926-5704; Tel: +81-55-926-5704

[c] *Division of Integrated Molecular Engineering, Chemical Resources Laboratory, Tokyo Institute of Technology, 4259 Nagatsuta-cho, Midori-ku, Yokohama, Kanagawa 226-8503, Japan.*

1. Experiments.

1.1. General information.

Reagents and solvents of best grade available were purchased from commercial suppliers and were used without further purification unless otherwise noted. Dried *N*,*N*-dimethylformamide (DMF) was obtained by distillation from CaH_2 under a reduced pressure. Dried triethylamine (NEt_3) was obtained by distillation from CaH_2 under a N_2 atmosphere after being stirred with KOH for overnight. Dried tetrahydrofuran (THF) was obtained by distillation from Na and benzophenone under a N_2 atmosphere.

Nuclear magnetic resonance (NMR) spectra were recorded on an AVANCE III 600 spectrometer (Bruker, Germany). The resonance frequencies are 600 and 151 MHz for ^{1}H and ^{13}C, respectively. Chemical shifts were reported as δ values in ppm relative to tetramethylsilane. High-resolution fast atom bombardment mass spectra (HR-FAB-MS) were measured with 3-nitrobenzyl alcohol (NBA) as a matrix and recorded on an LMS-HX-110 spectrometer (JEOL, Japan). Ultraviolet–visible (UV–vis) absorption and fluorescence spectra were recorded on an UV-2500PC or a RF-5300PC spectrometer (Shimadzu, Japan), respectively. Infrared (IR) absorption spectra were recorded on a FTS6000 spectrophotometer (Bio-Rad, USA). Differential scanning calorimetry (DSC) measurements were carried out at a rate of 10.0 °C/min under a N_2 atmosphere by using an EXSTAR X-DSC7000 calorimeter (Hitachi High-Tech Science, Japan).

1.2. Characterization of the films.

Atomic force microscopy (AFM) measurement was carried out to observe the topographies of the thin films by using a Cypher scanning probe microscope (Asylum Research, USA) in an AC mode (*i.e.* tapping mode) with an AC55TS or an AC160TS micro cantilever (Olympus, Japan).

Grazing incidence small-angle X-ray scattering (GISAXS) was measured using a Nano-Viewer setup with a two-dimensional detector PILATUS (Rigaku, Japan). The X-ray experiment was performed using a Cu Kα radiation beam (λ = 1.541 Å), which was converged and monochromatized by a Confocal Max Flax (CMF) mirror. The X-ray generator was a Micro7 rotating anode generator (Rigaku, Japan). The output current and voltage were set for 40 kV and 30 mA, respectively. The diameter of the X-ray beam controlled by a three-slit optical system was set to 250 μm. The incidence angle of the X-ray was set to *ca.* 0.2° to obtain in-plane signals effectively. Details can be found in ref. S1.

Transmission electron microscopy (TEM), high angle annular dark-field scanning transmission electron microscopy (HAADF-STEM) observations and energy dispersive X-ray (EDX) spectroscopy analyses were carried out by using a JEM-2100 (JEOL, Japan) with dry SD30GV (JEOL, Japan) detector. The acceleration voltage was 200 kV.

1.3. Thermodynamics measurement.

Differential scanning calorimetry (DSC) measurements were carried out at a rate of 10.0 °C/min under a N_2 atmosphere by using an EXSTAR X-DSC7000 calorimeter (Hitachi High-Tech Science, Japan). The samples were prepared by drying of $CHCl_3$ solutions of PEO_m-*b*-$PMA(Az)_n$ with $C_{60}\subset Zn_2$-CPD_{Ph}(TEO) on aluminium pans.

1.4. Sample preparation.

A series of PEO_m-*b*-$PMA(Az)_n$ block copolymers were systematically synthesized using atom transfer radical polymerization (ATRP) from a PEO_m macroinitiator (m = 114 or 272) based on our previous work.[S2] The molecular weight (M_w) and polydispersity (M_w/M_n) were determined from ^{1}H NMR and GPC measurements, respectively.

The mixed films were prepared by the spin coating on $CHCl_3$ washed-quartz plates or flesh surfaces of mica substrates from $CHCl_3$ solutions of PEO_m-*b*-$PMA(Az)_n$ with Zn_2-CPD_{Ph}(TEO) or $C_{60}\subset Zn_2$- CPD_{Ph}(TEO) for 30 sec at rates of 1000 rpm or 2000 rpm for GISAXS or except GISAXS, respectively. The concentration of PEO_m-*b*-$PMA(Az)_n$ was 1/100 (g/mL). The film thicknesses were *ca.* 130 (1000 rpm) and 100 nm (2000 rpm). The thermal annealing was carried out at 140 °C for 2 hours in vacuo. After heating, the films were cooled to 120 °C slowly over *ca.* 20 min in vacuo and then cooled to room temperature rapidly under an air atmosphere.

The samples for TEM analysis were prepared subject to the following procedure. The thermal annealed mixed films on mica substrates easily peeled from the substrates by soaked in water, transferred onto supporting memblene-coated Mo micro-grids (Nissin EM, Japan), and then exposed on RuO_4 vapor using 0.5 wt% RuO_4 aqueous solution at room temperature.

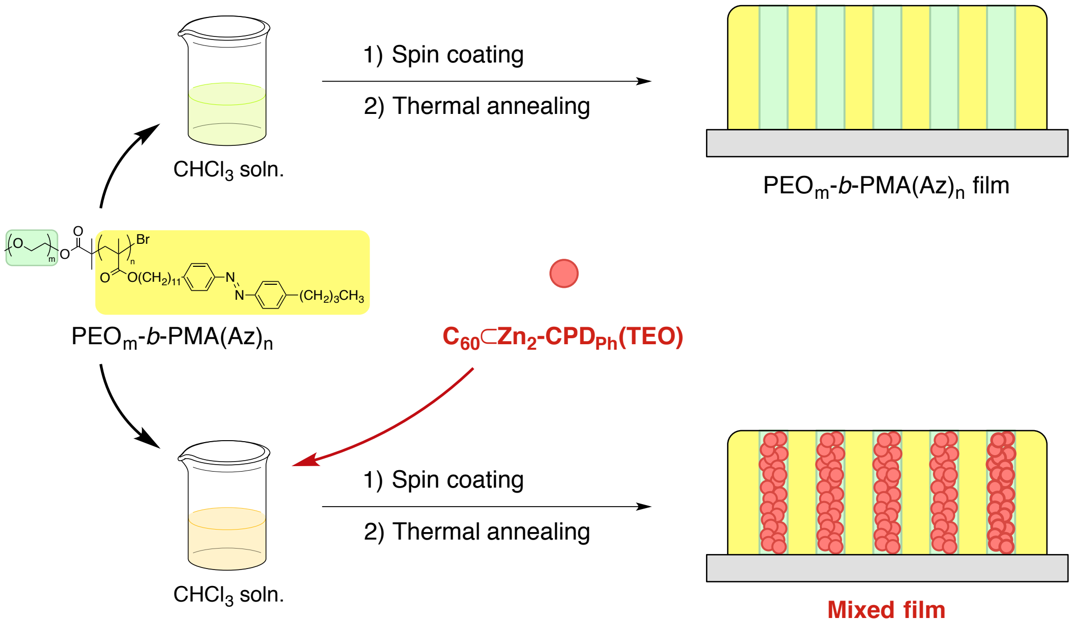

Scheme S1. Schematic illustration of the mixed film preparation.

2. Synthesis.

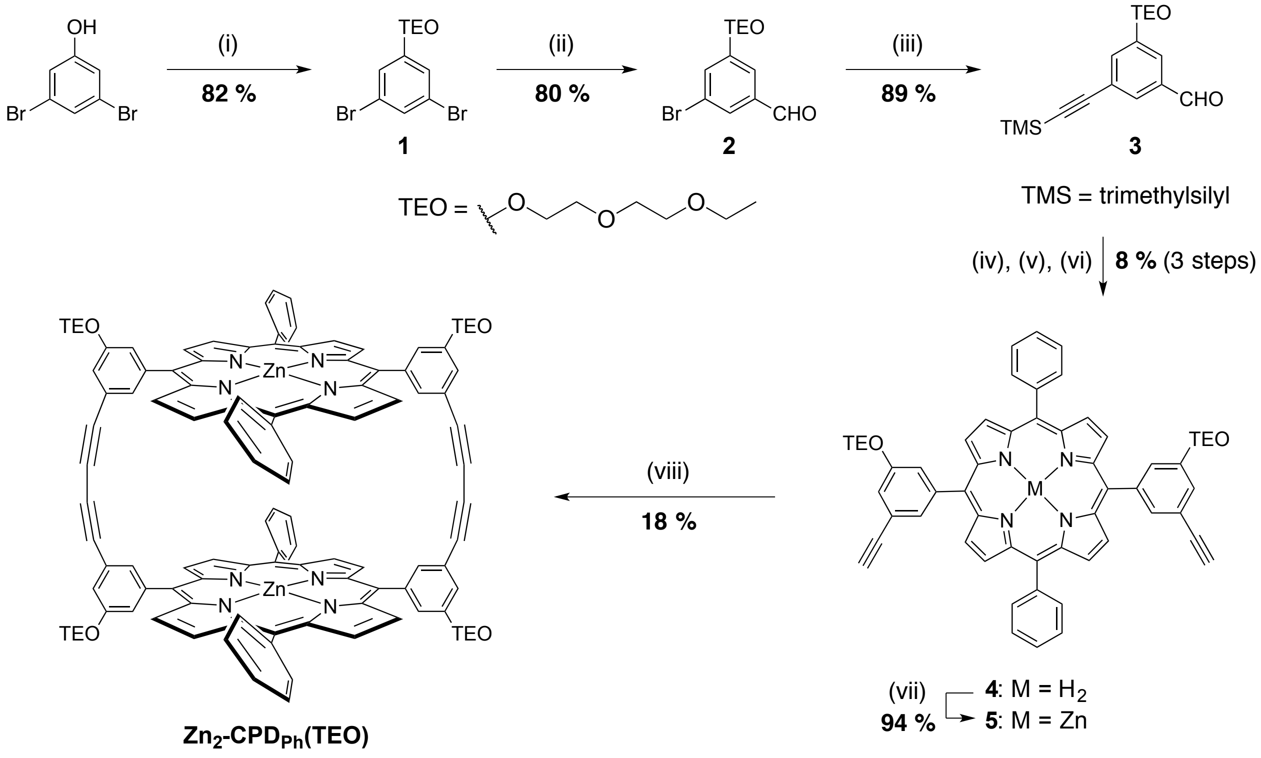

Scheme S2. Synthetic pathway for Zn_2-CPD_{Ph}(TEO). (i) 1-Bromo-2-(2-ethoxyethoxy)ethane, K_2CO_3, 2-butanone; (ii) *n*-butyllithium, DMF, THF; (iii) trimethylsilylacetylene, $Pd(OAc)_2$, PPh_3, NEt_3; (iv) *meso*-phenyldipyrromethane, zinc *p*-*tert*-butylbenzoate, TFA, DDQ, CH_2Cl_2; (v) $KF{\cdot}2H_2O$, DMF; (vi) TFA, $CHCl_3$; (vii) $Zn(OAc)_2{\cdot}2H_2O$, CH_2Cl_2 and (viii) CuCl, pyridine, air.

2.1. 1,3-Dibromo-5-[2-(2-ethoxyethoxy)ethoxy]benzene (1).

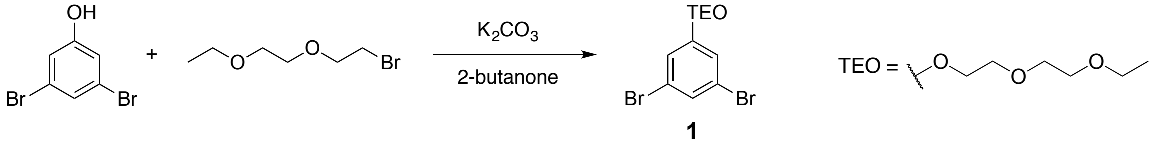

3,5-Dibromophenol[S3] (23.1 g, 91.7 mmol), 1-bromo-2-(2-ethoxyethoxy)ethane[S4] (15.8 g, 80.2 mmol), and ground K_2CO_3 (28 g, 0.20 mol) were refluxed in 2-butanone (200 mL) under a N_2 atmosphere for 24 hours. After confirming the disappearance of 1-bromo-2-(2-ethoxyethoxy)ethane by ^{1}H NMR, 1-bromohexane (4.2 mL, 30 mmol) was added and the reaction mixture was refluxed again for 2 hours. The resulted mixture was poured to water (500 mL) and extracted with CH_2Cl_2 (150 mL × 3). Combined organic layer was dried over Na_2SO_4 and then evaporated. The crude product was purified by column chromatography (silica-gel, *n*-hexane/acetone = 10/1) to give the target compound as an orange oil (24.1 g, 82 %).

^{1}H NMR (DMSO-d_6, 600 MHz): δ 1.09 (t, J = 7.2 Hz, 3H, $-O(CH_2CH_2O)_2CH_2C\underline{H_3}$), 3.42 (q, J = 7.2 Hz, 2H, $-O(CH_2CH_2O)_2C\underline{H_2}CH_3$), 3.48 (t, J = 4.8 Hz, 2H, $-O(CH_2)_2OCH_2C\underline{H_2}OC_2H_5$), 3.56 (t, J = 4.8 Hz, 2H, $-O(CH_2)_2OC\underline{H_2}CH_2OC_2H_5$), 3.71 (t, J = 4.8 Hz, 2H, $-OCH_2C\underline{H_2}O(CH_2)_2OC_2H_5$), 4.15 (t, J = 4.2 Hz, 2H, $-OC\underline{H_2}CH_2O(CH_2)OC_2H_5$), 7.21 (d, J = 1.2 Hz, 2H, Ar–H), 7.37 (br-s, 1H, Ar–H); ^{13}C NMR (DMSO-d_6, 151 MHz): δ 15.1, 65.6, 68.1, 68.7, 69.2, 69.9, 117.1, 122.8, 125.6, 160.1; HR-FAB-MS (NBA): *m*/*z* calcd for $C_{12}H_{17}Br_2O_3$: 366.9544; found: 366.9582; IR (oil): ν = 3079, 2974, 2929, 2878, 2360, 1585, 1559, 1437, 1420, 1298, 1257, 1232, 1112, 1058, 988, 956, 832, 744, 669 cm^{-1}.

2.2. 3-Bromo-5-[2-(2-ethoxyethoxy)ethoxy]benzaldehyde (2).

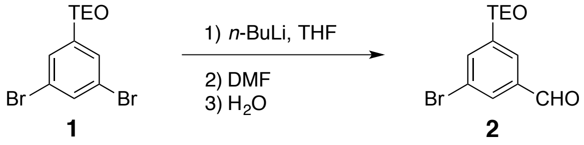

The dibromide **1** (12.3 g, 33.4 mmol) was added into a three-necked flask and the flask was charged with N_2. Then, dried THF (330 mL) was added into the flask under a N_2 atmosphere and the resulted solution was cooled to –78 °C. To this solution, *n*-butyllithium (2.69 M solution in *n*-hexane, 12.4 mL, 33.4 mmol) was added dropwise over few minutes. An hour later, excess dried DMF (20 mL, 0.26 mol) was added to the resulted mixture. After warming the solution to room temperature, the reaction mixture was quenched with water, poured to water, and extracted with $CHCl_3$ (100 mL × 2). Combined organic layer was dried over Na_2SO_4 and then evaporated. The crude product was purified by column chromatography (silica-gel, *n*-hexane/EtOAc = 3/1) to give the target compound as a yellow oil (8.50 g, 80 %).

^{1}H NMR (DMSO-d_6, 600 MHz): δ 1.09 (t, J = 7.2 Hz, 3H, –$O(CH_2CH_2O)_2CH_2C\underline{H_3}$), 3.42 (q, J = 7.2 Hz, 2H, –$O(CH_2CH_2O)_2C\underline{H_2}CH_3$), 3.49 (t, J = 4.8 Hz, 2H, –$O(CH_2)_2OCH_2C\underline{H_2}OC_2H_5$), 3.58 (t, J = 4.8 Hz, 2H, –$O(CH_2)_2OC\underline{H_2}CH_2OC_2H_5$), 3.75 (t, J = 4.8 Hz, 2H, –$OCH_2C\underline{H_2}O(CH_2)_2OC_2H_5$), 4.21 (t, J = 4.8 Hz, 2H, –$OC\underline{H_2}CH_2O(CH_2)OC_2H_5$), 7.46 (br-s, 1H, Ar-H), 7.52 (br-s, 1H, Ar–H), 7.65 (br-s, 1H, Ar–H), 9.93 (s, 1H, –CHO); ^{13}C NMR (DMSO-d_6, 600 MHz): δ 15.1, 65.6, 68.1, 68.7, 69.2, 70.0, 114.1, 122.9, 123.3, 124.4, 138.8, 159.9, 191.8; HR-FAB-MS (NBA): *m*/*z* calcd for $C_{13}H_{18}BrO_4$: 317.0388; found: 317.0356; IR (oil): ν = 3385, 3076, 2974, 2930, 2876, 2727, 2362, 1702, 1592, 1571, 1448, 1385, 1317, 1272, 1113, 1060, 994, 948, 886, 849, 795, 691 cm^{-1}.

2.3. 3-[2-(2-Ethoxyethoxy)ethoxy]-5-[2-(trimethylsilyl)ethynyl]benzaldehyde (3).

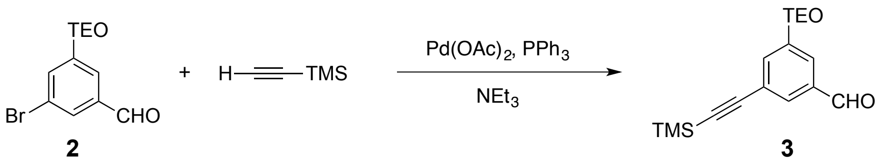

A solution of **2** (9.58 g, 30.2 mmol), palladium(II) acetate (68 mg, 0.30 mmol), and triphenyl phosphine (0.17 g, 0.66 mmol) in dried triethylamine (30 mL) was degassed with a stream of N_2 for 30 min. Then, trimethylsilylacetylene (6.2 mL, 45 mmol) was added. The mixture was heated rapidly to 80 °C, and then stirred for 18 hours under a N_2 atmosphere. The resulted mixture was cooled to room temperature and the white precipitation was removed by filtration. The dark brown filtrate was evaporated and then purified by column chromatography (silica-gel, *n*-hexane/EtOAc = 3/1) to furnish the product as a thick brown oil (9.01 g, 89 %).

^{1}H NMR (DMSO-d_6, 600 MHz): δ 0.25 (s, 9H, $–Si(C\underline{H}_3)_3$), 1.09 (t, J = 7.2 Hz, 3H, $–O(CH_2CH_2O)_2CH_2C\underline{H}_3$), 3.42 (q, J = 7.2 Hz, 2H, $–O(CH_2CH_2O)_2C\underline{H}_2CH_3$), 3.48 (t, J = 4.8 Hz, 2H, $–O(CH_2)_2OCH_2C\underline{H}_2OC_2H_5$), 3.58 (t, J = 4.8 Hz, 2H, $–O(CH_2)_2OC\underline{H}_2CH_2OC_2H_5$), 3.75 (t, J = 4.8 Hz, 2H, $–OCH_2C\underline{H}_2O(CH_2)_2OC_2H_5$), 4.20 (t, J = 4.8 Hz, 2H, $–OC\underline{H}_2CH_2O(CH_2)OC_2H_5$), 7.32–7.33 (m, 1H, Ar-H), 7.44–7.45 (m, 1H, Ar–H), 7.57 (t, J = 1.2 Hz, 1H, Ar–H), 9.95 (s, 1H, –CHO); ^{13}C NMR (DMSO-d_6, 151 MHz): δ –0.3, 15.1, 65.6, 67.9, 68.8, 69.2, 70.0, 95.6, 103.6, 115.2, 122.7, 124.2, 125.7, 137.8, 159.0, 192.3; HR-FAB-MS (NBA): *m*/*z* calcd for $C_{18}H_{27}O_4Si$: 335.1679; found: 335.1674; IR (oil): ν = 3387, 2962, 2872, 2728, 2340, 2330, 2162, 1705, 1588, 1457, 1384, 1330, 1299, 1251, 1169, 1117, 1067, 847, 794, 763, 679 cm^{-1}.

2.4. 5,15-Di{3-[2-(2-ethoxyethoxy)ethoxy]-5-ethynylphenyl}-10,20-diphehylporphine (4).

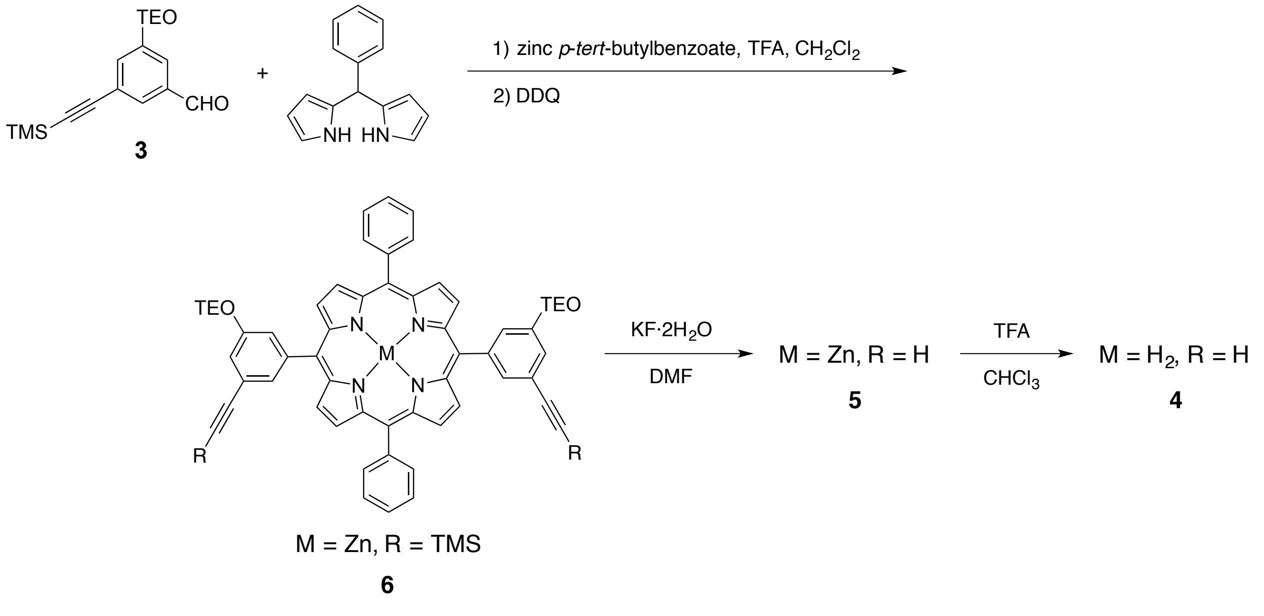

A solution of **3** (1.03 g, 3.08 mmol), *meso*-phenyldipyrromethane[S5] (667 mg, 3.00 mmol), and zinc *p-tert*-butylbenzoate (2.52 g, 6.00 mmol) in CH_2Cl_2 (600 mL) was degassed with a stream of N_2 for 40 min. To the solution, trifluoroacetic acid (0.54 mL, 7.2 mmol) was added and stirred under a N_2 atmosphere under a dark. After 3 hours, 2,3-dichloro-5,6-dicyano-1,4-benzoquinone (1.02 g, 4.49

mmol) was added and the mixtures was stirred for an hour. After neutralization with NEt_3 (1.2 mL, 7.5 mmol), the resulted mixture was diluted with $CHCl_3$ (300 mL), poured to water (500 mL), and then extracted with $CHCl_3$ (200 mL × 2). Combined organic layer was dried over Na_2SO_4 and then evaporated. The scrambled porphyrin derivatives were removed by column chromatography (silica-gel, $CHCl_3$/EtOAc = 50/1 to 1/1) and then flash column chromatography (silica-gel, $CHCl_3$) gave the crude {5,15-bis{3-[2-(2-ethoxyethoxy)ethoxy]-5-[2-(trimethylsilyl)ethynyl]phenyl}-10,20-diphehylporphininato}zinc(II) (**6**) as a purple solid.

To remove the trimethylsilyl groups, the crude **6** and $KF\cdot 2H_2O$ (0.25 g, 2.7 mmol) were dissolved in DMF (15 mL), and the solution was stirred overnight under a N_2 atmosphere. The resulted mixture was diluted with benzene (200 mL) and then washed with water (150 mL × 3). The organic layer was dried over Na_2SO_4 and then evaporated to give the crude {5,15-bis{3-[2-(2-ethoxyethoxy)ethoxy]-5-ethynylphenyl}-10,20-diphehyl-porphinato}zinc(II) (**5**) as a purple solid.

To remove the zinc ions of the porphyrin, trifluoroacetic acid (3.5 mL, 47 mmol) was added to the solution of the crude **5** in $CHCl_3$ (100 mL) and then stirred under a N_2 atmosphere for an hour. After quenching with NEt_3 (10 mL, 72 mmol), the resulted mixture was diluted with $CHCl_3$ (50 mL) and then washed with water (200 mL × 2). The organic layer was dried over Na_2SO_4 and then evaporated. The residue was purified by column chromatography (Al_2O_3, $CHCl_3$) and then recrystallized from CH_2Cl_2/MeOH to give the terminal acetylene-substituted free-base porphyrin monomer **4** as a purple powder (118 mg, 8 %).[S6]

^1H NMR ($CDCl_3$, 600 MHz): δ –2.80 (br-s, 2H, –NH), 1.22 (t, J = 7.2 Hz, 6H, $-O(CH_2CH_2O)_2CH_2C\underline{H_3}$), 3.18 (s, 2H, $-C{\equiv}CH$), 3.55 (q, J = 7.2 Hz, 4H, $-O(CH_2CH_2O)_2C\underline{H_2}CH_3$), 3.66 (t, J = 4.8 Hz, 2H, $-O(CH_2)_2OCH_2C\underline{H_2}OC_2H_5$), 3.79 (t, J = 4.8 Hz, 2H, $-O(CH_2)_2OC\underline{H_2}CH_2OC_2H_5$), 3.99 (t, J = 4.8 Hz, 2H, $-OCH_2C\underline{H_2}O(CH_2)_2OC_2H_5$), 4.38 (t, J = 4.8 Hz, 2H, –OC$\underline{H_2}$CH$_2$O(CH$_2$)OC$_2$H$_5$), 7.52 (s, 2H, Ar-H), 7.79–7.84 (m, 8H, Ar–H), 8.01 (s, 2H, Ar–H), 8.25 (d, *J* = 7.2 Hz, 4H, Ar-H), 8.90 (br-s, 8H, pyrrole β–H); ^{13}C NMR (CDCl$_3$, 151 MHz): δ 15.3, 66.9, 68.1, 69.9, 70.0, 71.2, 83.8, 117.6, 118.8, 120.5, 121.4, 122.6, 126.9, 127.9, 131.3, 134.7, 142.1, 143.7, 157.1; HR-FAB-MS (NBA): *m*/*z* calcd for $C_{60}H_{54}O_6N_4$: 926.4043; found: 926.4038; UV–vis (CHCl$_3$): λ_{max} (ε, cm^{-1} M^{-1}) = 420 (401000), 516 (17000), 550 (6200), 590 (5100), 645 (2900) nm; IR (KBr): ν = 3291, 3238, 2971, 2921, 2867, 1581, 1474, 1441, 1420, 1351, 1320, 1296, 1242, 1194, 1173, 1113, 1066, 1031, 1000, 972, 921, 869, 802, 760, 733, 702, 659 cm^{-1}.

2.5. {5,15-Di{3-[2-(2-ethoxyethoxy)ethoxy]-5-ethynylphenyl}-10,20-diphehylporphinato}-zinc(II) (5).

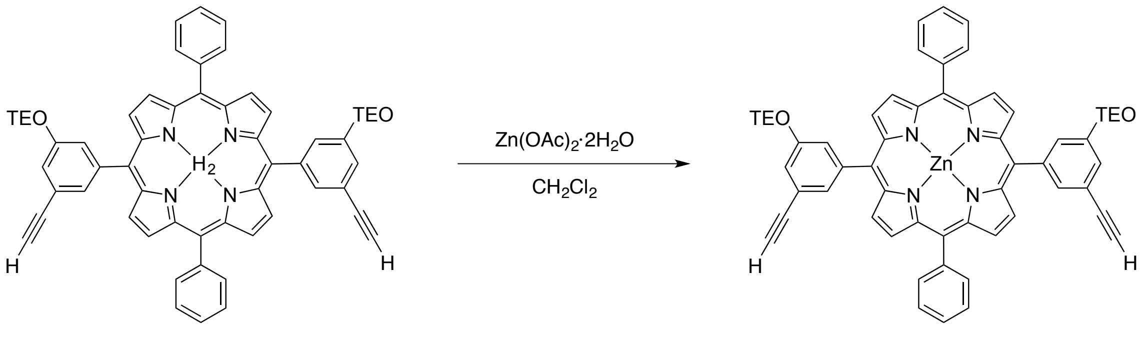

4 **5**

Zn(OAc)$_2$·2H$_2$O (0.12 g, 0.50 mmol) dissolved in MeOH (2 mL) was added to a solution of **4** (49 mg, 50 μmol) in CH$_2$Cl$_2$ (50 mL). The resulted solution was refluxed under a N$_2$ atmosphere for 2 hours and then cooled to room temperature. The reaction mixture was diluted with CH$_2$Cl$_2$ (100 mL), washed with water (100 mL × 3), dried over Na$_2$SO$_4$, and then evaporated. The residue was purified by column chromatography (silica-gel, CHCl$_3$/EtOAc = 100/1 v/v). The combined eluate was evaporated to give the product as a purple solid (48 mg, 92 %).

^{1}H NMR (CDCl$_3$, 600 MHz): δ 1.16 (t, *J* = 7.2 Hz, 6H, –O(CH$_2$CH$_2$O)$_2$CH$_2$C$\underline{H_3}$), 3.12 (s, 2H, –C≡CH), 3.50 (q, *J* = 7.2 Hz, 4H, –O(CH$_2$CH$_2$O)$_2$C$\underline{H_2}$CH$_3$), 3.60 (t, *J* = 4.8 Hz, 4H, –

$O(CH_2)_2OCH_2C\underline{H_2}OC_2H_5$), 3.74 (t, J = 4.8 Hz, 4H, $-O(CH_2)_2OC\underline{H_2}CH_2OC_2H_5$), 3.93 (t, J = 4.8 Hz, 4H, $-OCH_2C\underline{H_2}O(CH_2)_2OC_2H_5$), 4.33 (t, J = 4.8 Hz, 4H, $-OC\underline{H_2}CH_2O(CH_2)OC_2H_5$), 7.47 (s, 2H, Ar–H), 7.74–7.80 (m, 8H, Ar–H), 7.96 (br-s, 2H, Ar–H), 8.21 (d, J = 7.8 Hz, 4 H, Ar–H), 8.94–8.95 (m, 8H, pyrrole β–H); ^{13}C NMR ($CDCl_3$, 151 MHz): δ 15.2, 66.8, 68.1, 69.9, 70.0, 71.1, 83.9, 117.5, 119.8, 121.2, 121.5, 122.4, 126.7, 127.7, 131.3, 132.0, 132.4, 134.6, 134.6, 134.6, 142.8, 144.4, 150.0, 150.5, 157.0; HR-FAB-MS (NBA): m/z calcd for $C_{60}H_{52}O_6N_4Zn$: 988.3178; found: 988.3218; UV–vis (THF): λ_{max} (ε, cm^{-1} M^{-1}) = 425 (593000), 556 (22000), 595 (6300) nm; IR (KBr): ν = 3441, 3286, 2971, 2925, 2869, 1580, 1486, 1419, 1342, 1180, 1112, 1071, 1002, 938, 872, 820, 799, 767, 720, 702, 663 cm^{-1}.

2.6. **Zn_2-CPD_{Ph}(TEO).**

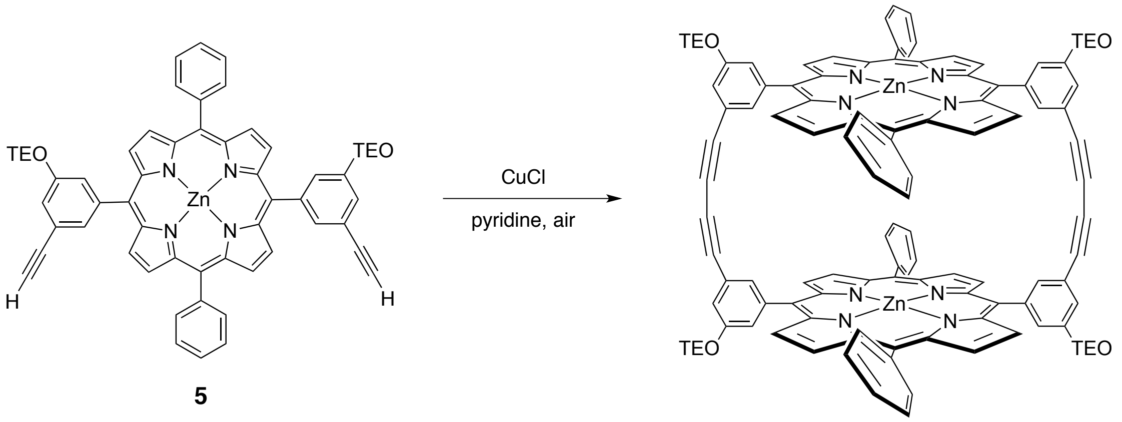

5

Zn_2-CPD_{Ph}(TEO)

Copper(I) chloride (4.0 g, 40 mmol) was added to a solution of **5** (135 mg, 0.136 mmol) in pyridine (600 mL) with continuous stirring. The reaction mixture was stirred overnight at 80 °C under an air atmosphere. After cooling to room temperature, aqueous ammonia (14 %, 200 mL) was added and then O_2 was bubbled into the mixture for 30 min. The resultant mixture was diluted with $CHCl_3$ (300 mL), washed with aqueous ammonia (14 %, 300 mL × 2), dried over Na_2SO_4, and then the solvent was evaporated. The purple residue was purified by GPC (Bio-Beads®, $CHCl_3$) and then recrystallized from CH_2Cl_2/MeOH to give the product as a purple powder (24 mg, 18 %).

^{1}H NMR ($CDCl_3$, 600 MHz): δ 1.18 (t, J = 7.2 Hz, 12H, $–O(CH_2CH_2O)_2CH_2C\underline{H_3}$), 3.52 (q, J = 7.2 Hz, 4H, $–O(CH_2CH_2O)_2C\underline{H_2}CH_3$), 3.63 (t, J = 4.8 Hz, 2H, $–O(CH_2)_2OCH_2C\underline{H_2}OC_2H_5$), 3.76 (t, J = 4.6 Hz, 2H, $–O(CH_2)_2OC\underline{H_2}CH_2OC_2H_5$), 3.98 (t, J = 4.8 Hz, 2H, $–OCH_2C\underline{H_2}O(CH_2)_2OC_2H_5$), 4.39 (t, J = 4.8 Hz, 2H, $–OC\underline{H_2}CH_2O(CH_2)OC_2H_5$), 7.04 (s, 4H, Ar–H), 7.21 (s, 4H, Ar–H), 7.65 (t, J = 7.2 Hz, 4H, Ar–H), 7.70–7.76 (m, 8H, Ar–H), 7.94 (d, J = 6.6 Hz, 4H, Ar–H), 8.07 (d, J = 6.6 Hz, 4H, Ar–H), 8.17 (s, 4H, Ar–H), 8.73–8.75 (m, 16H, pyrrole β–H); ^{13}C NMR ($CDCl_3$, 151 MHz): δ 15.3, 66.9, 68.2, 70.0, 70.0, 71.2, 74.5, 83.6, 114.4, 119.0, 120.2, 120.5, 121.2, 126.6, 127.6, 131.8, 132.3, 134.4, 135.9, 142.6, 144.2, 149.6, 150.1, 157.5; HR-FAB-MS (NBA): *m*/*z* calcd for $C_{120}H_{100}O_{12}N_8Zn_2$: 1972.6044; found: 1972.6105; UV–vis (THF): $\lambda_{\max}$ (ε, cm^{-1} M^{-1}) = 424 (1015000), 557 (40000), 597 (10500) nm; IR (KBr): ν = 3436, 2971, 2928, 2871, 1579, 1415, 1323, 1296, 1229, 1197, 1178, 1112, 1069, 1003, 959, 872, 819, 720, 701 cm^{-1}.

3. Experimental data.

3.1. UV–vis absorption spectroscopy.

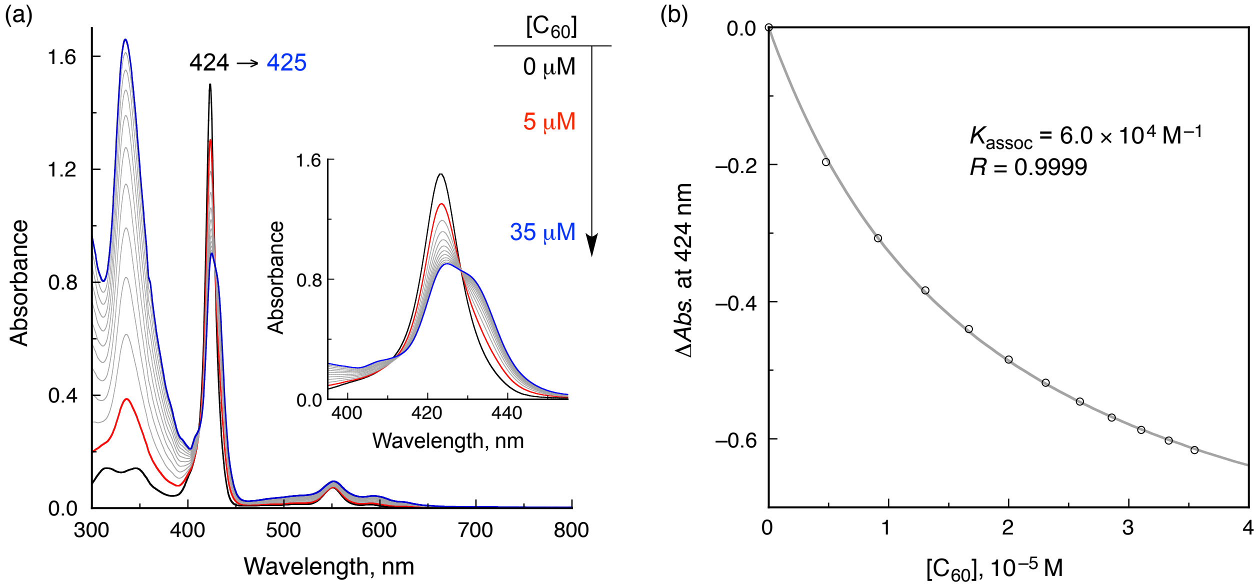

Figure S1. (a) UV–vis absorption changes of Zn_2-CPD_{Ph}(TEO) in the course of titration with C_{60} in toluene at 27 °C. [Zn_2-CPD_{Ph}(TEO)] = 2.0×10^{-6} M. The inset shows the Soret band region. (b) Changes in the UV–vis absorbance (Δ*Abs*) at 424 nm. The curve was fitted by using the equation in ref. 19 in the main text.

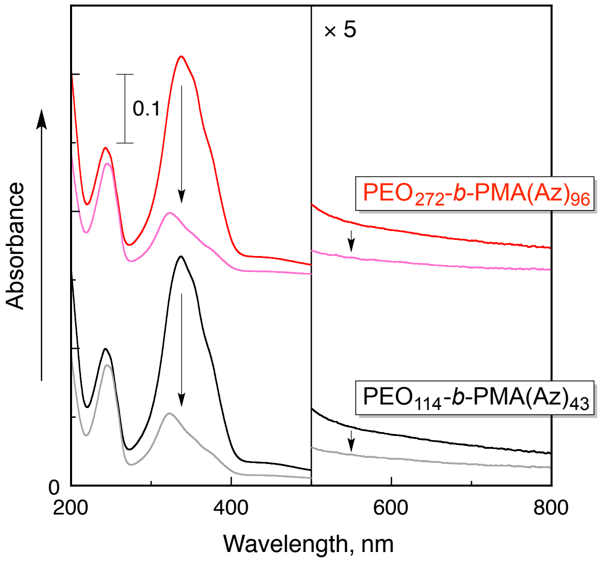

Figure S2. UV–vis absorption changes of (black) PEO$_{114}$-*b*-PMA(Az)$_{43}$ and (red) PEO$_{272}$-*b*-PMA(Az)$_{96}$ films by thermal annealing. Thicknesses of the films were 100 nm. Deep color: just after film preparation; light color: after thermal annealing.

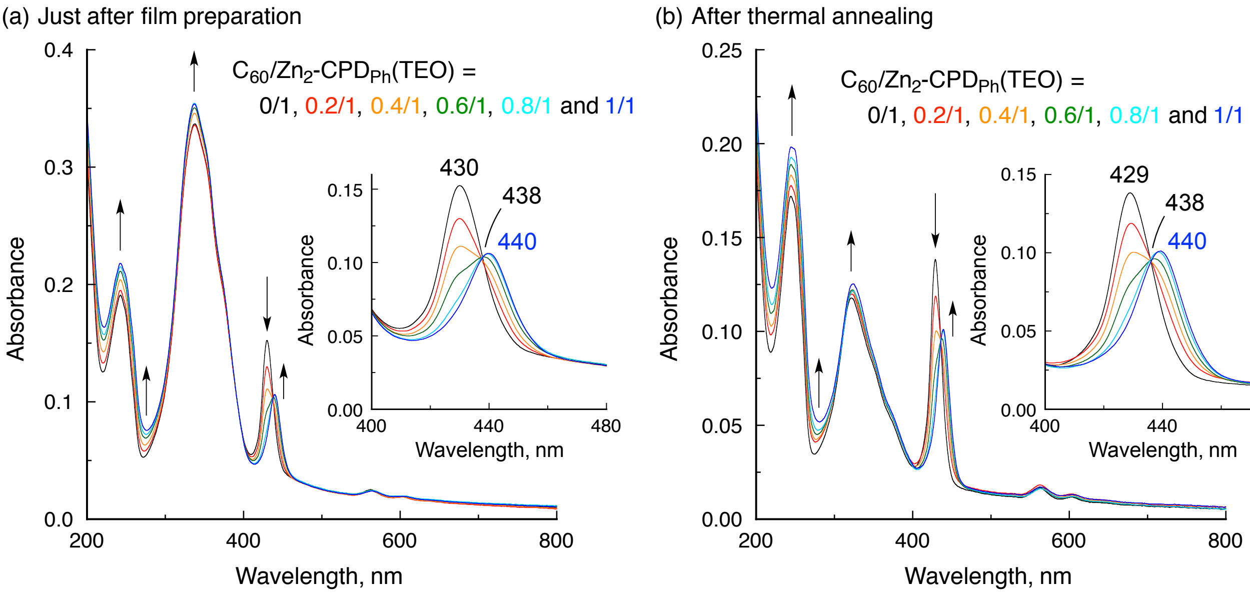

Figure S3. UV–vis absorption changes of the mixed films coated on quartz plates of Zn_2-CPD_{Ph}(TEO) with PEO_{114}-*b*-$PMA(Az)_{43}$ in the course of mixing of C_{60}. The insets show the Soret band region. (a) Just after film preparatrion and (b) after thermal annealing. The concentrations of Zn_2-CPD_{Ph}(TEO) were fixed so that {C_{60} + Zn_2-CPD_{Ph}(TEO)}/(PEO block) = 1/3 (w/w) when C_{60}/Zn_2-CPD_{Ph}(TEO) = 1/1 (mol/mol). Thicknesses of the films were 100 nm. The all spectral data were not corrected except background (an 1 mm thicknes quartz plate) adjustment.

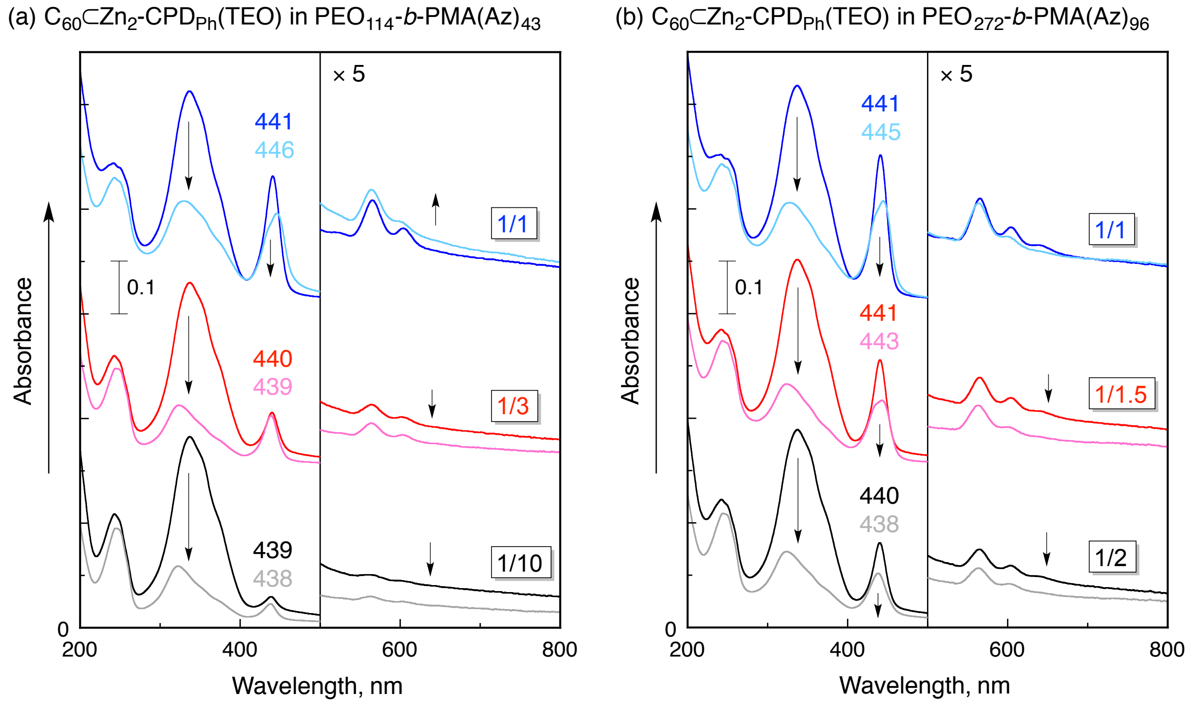

Figure S4. UV–vis absorption changes by thermal annealing of mixed films of C_{60}⊂Zn_2-CPD_{Ph}(TEO) with (a) PEO_{114}-*b*-PMA$(Az)_{43}$ and (b) PEO_{272}-*b*-PMA$(Az)_{96}$ that made by various content of C_{60}⊂Zn_2-CPD_{Ph}(TEO) and PEO block. Thicknesses of the films were 100 nm. Deep color: just after film preparation; light color: after thermal annealing. The contents are shown in the magnified spectra.

3.2. GISAXS measurement.

$C_{60}\subset Zn_2$-CPD$_{\mathrm{Ph}}$(TEO) in PEO$_{114}$-*b*-PMA(Az)$_{43}$ (content: 1/3)

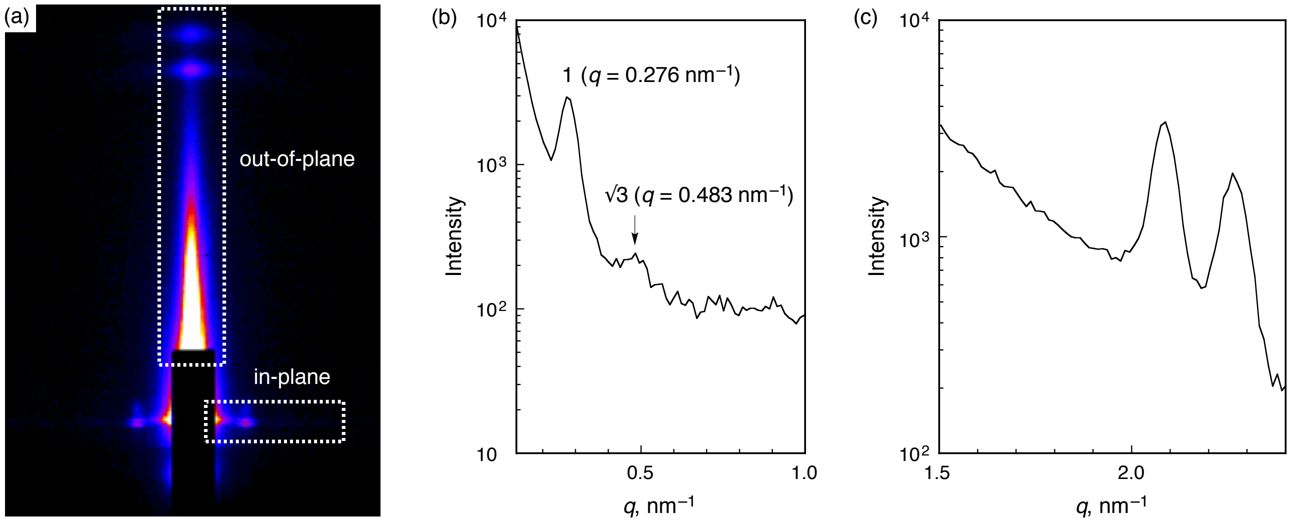

$C_{60}\subset Zn_2$-CPD$_{\mathrm{Ph}}$(TEO) in PEO$_{272}$-*b*-PMA(Az)$_{96}$ (content: 1/1.5)

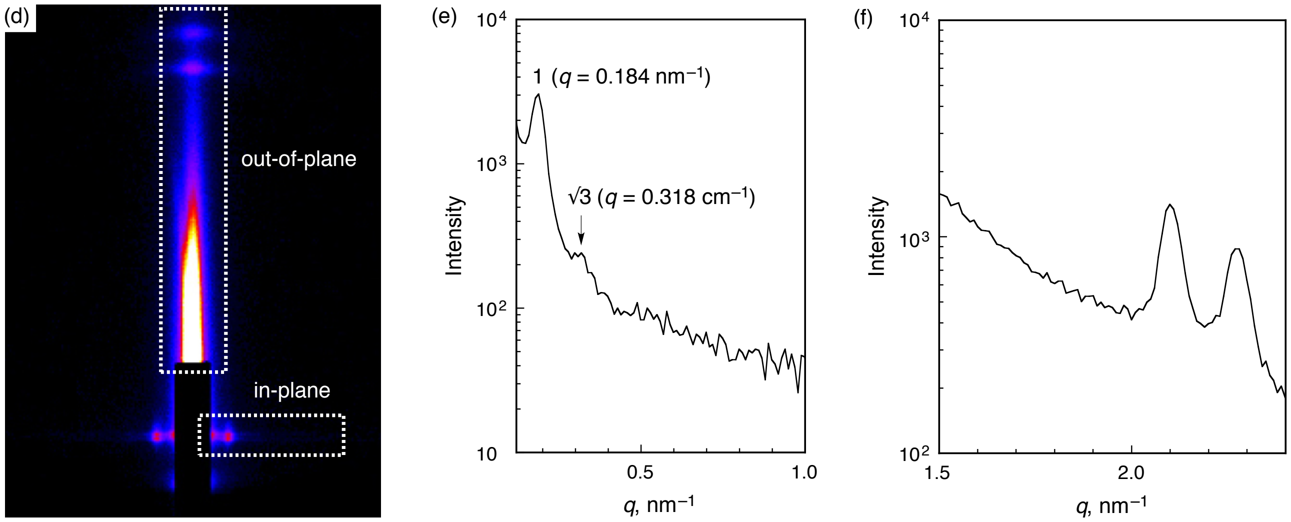

Figure S5. GISAXS (a,d) 2D images, (b,e) in-plane profiles and (c,f) out-of-plane profiles of the thermal annealed mixed films of $C_{60}\subset Zn_2$-CPD$_{\mathrm{Ph}}$(TEO) with (a–c) PEO$_{114}$-*b*-PMA(Az)$_{43}$ or (d–f) PEO$_{272}$-*b*-PMA(Az)$_{96}$. The contents are (a–c) 1/3 and (d–f) 1/1.5. Thicknesses of the films were 130 nm.

3.3. Electron microscopy analysis.

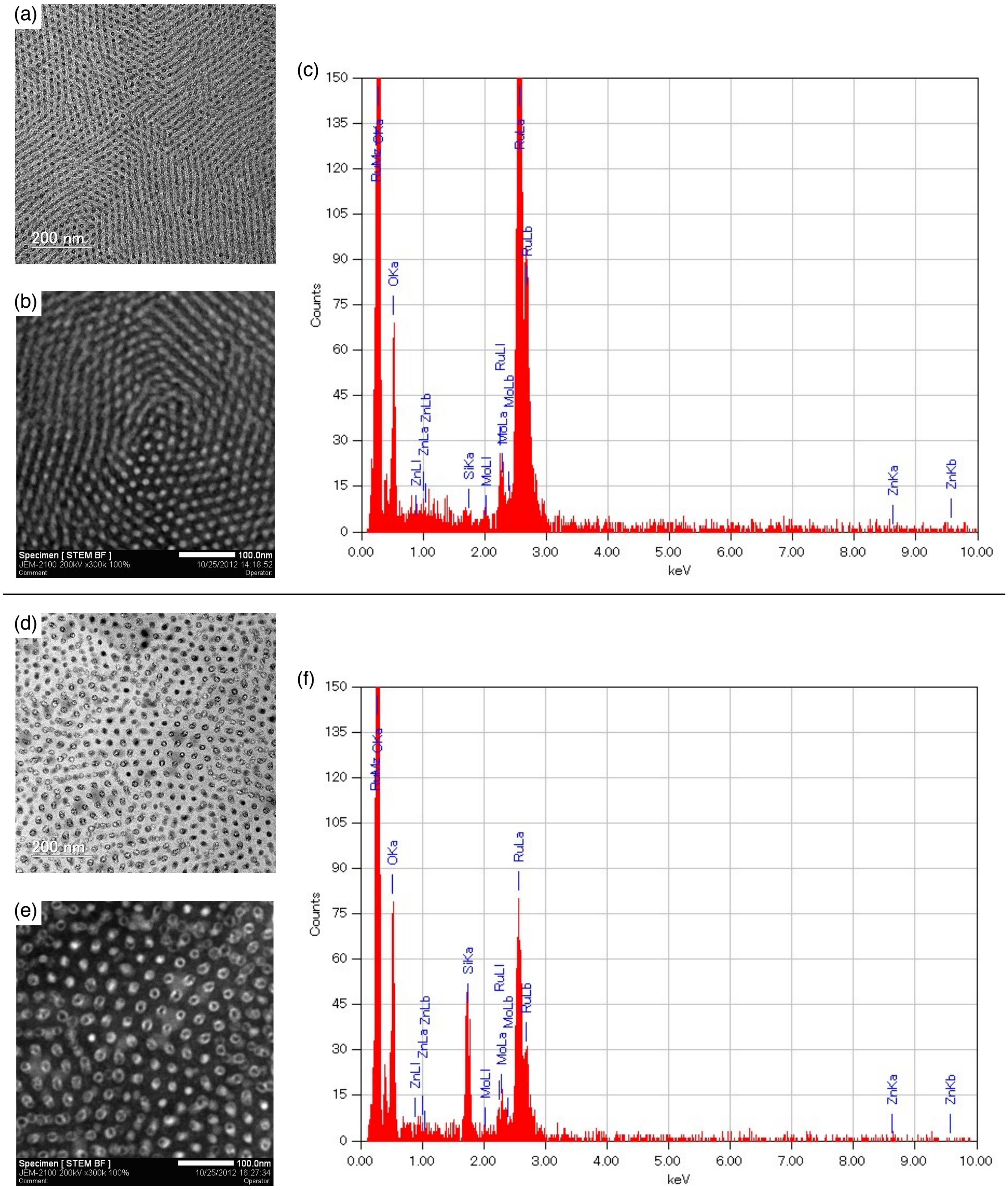

Figure S6. (a,d) TEM and (b,e) HAADF-STEM images, and (c,f) EDX spectra of the RuO_4 stained mixed films mounted on Mo micro-grids. Analytical areas of EDX spectra are identical with the fields of the corresponding HAADF-STEM images. The block copolymers: (a-c) PEO_{114}-*b*-$PMA(Az)_{43}$ and (d-f) PEO_{272}-*b*-$PMA(Az)_{96}$; the contents: (a-c) 1/3 and (d-f) 1/1; the acceleration voltage: 200 kV.

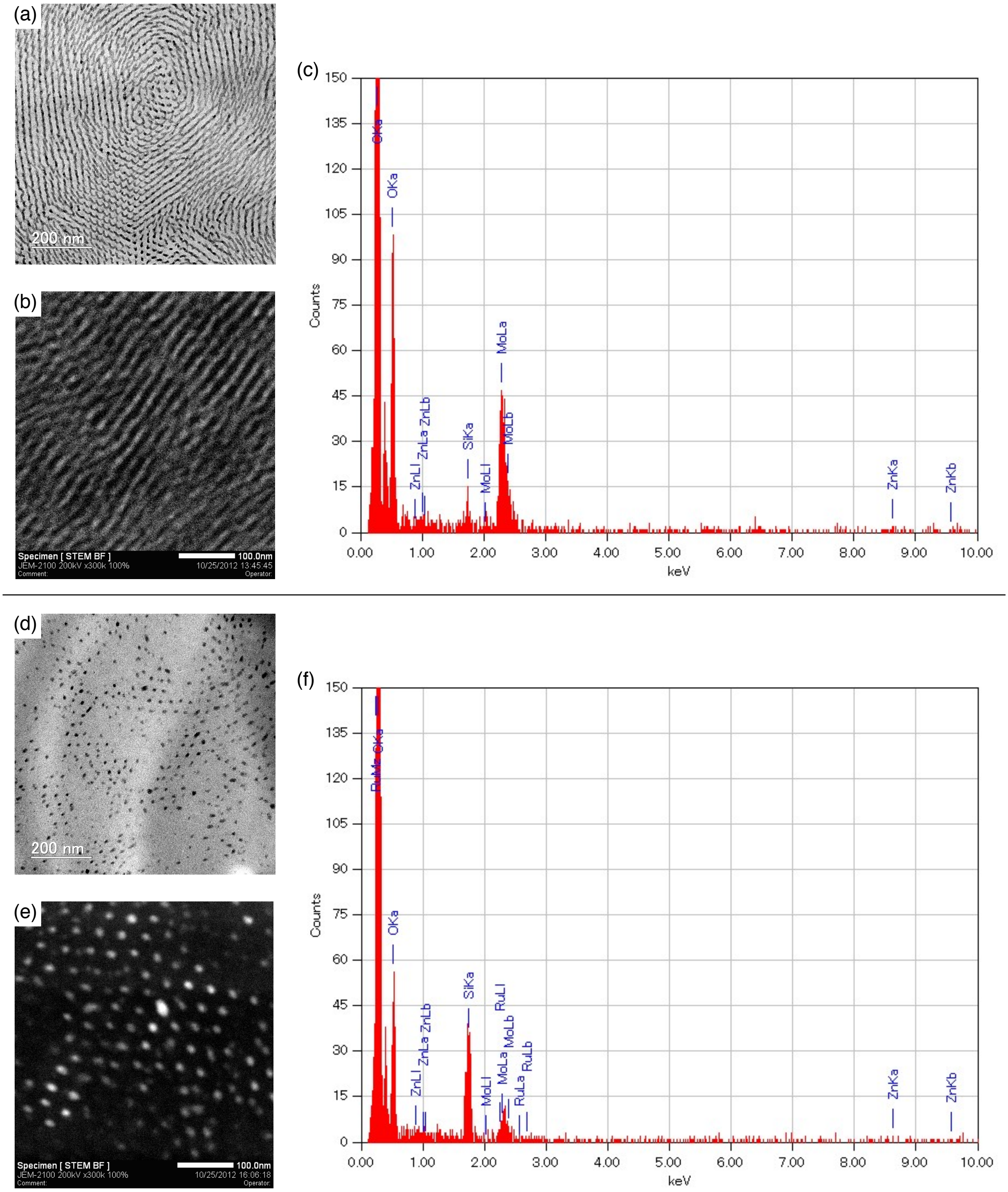

Figure S7. (a,d) TEM and (b,e) HAADF-STEM images, and (c,f) EDX spectra of the unstained mixed films mounted on Mo micro-grids. Analytical areas of EDX spectra are identical with the fields of the corresponding HAADF-STEM images. The block copolymers: (a-c) PEO_{114}-*b*-$PMA(Az)_{43}$ and (d-f) PEO_{272}-*b*-$PMA(Az)_{96}$; the contents: (a-c) 1/3 and (d-f) 1/1; the acceleration voltage: 200 kV.

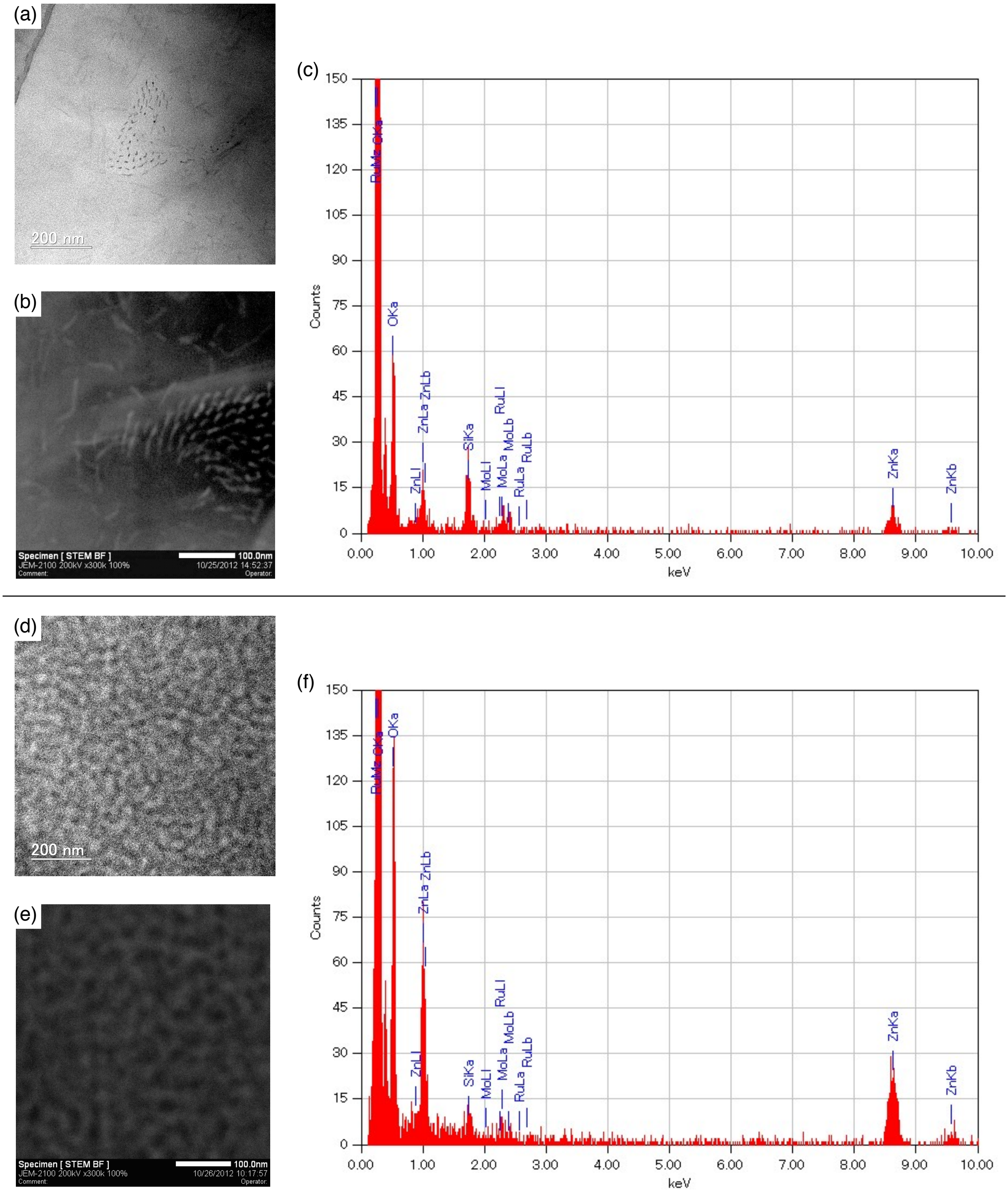

Figure S8. (a,d) TEM and (b,e) HAADF-STEM images, and (c,f) EDX spectra of the RuO_4 stained mixed films mounted on Mo micro-grids. Analytical areas of EDX spectra are identical with the fields of the corresponding HAADF-STEM images. The block copolymers: (a-c) PEO_{114}-*b*-$PMA(Az)_{43}$ and (d-f) PEO_{272}-*b*-$PMA(Az)_{96}$; the contents: (a-c) 10/3 and (d-f) 10/1; the acceleration voltage: 200 kV.

3.4. Thermal analysis.

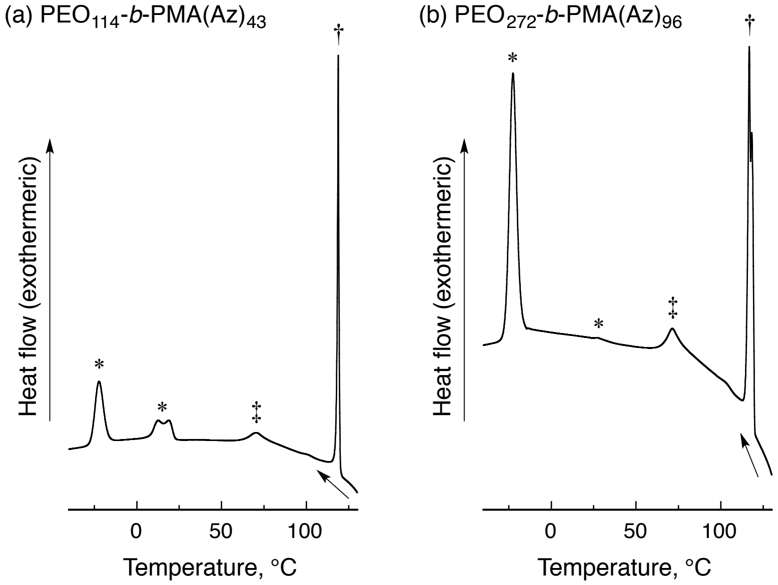

Figure S9. DSC 1st cooling curves of a) PEO$_{114}$-*b*-PMA(Az)$_{43}$ and b) PEO$_{272}$-*b*-PMA(Az)$_{96}$. The cooling rate was 10.0 °C/min. † and ‡ denote the Iso → SmA and SmC → SmX transition of the PMA(Az) matrix, respectively. * denotes the freezing transition of the PEO domain.

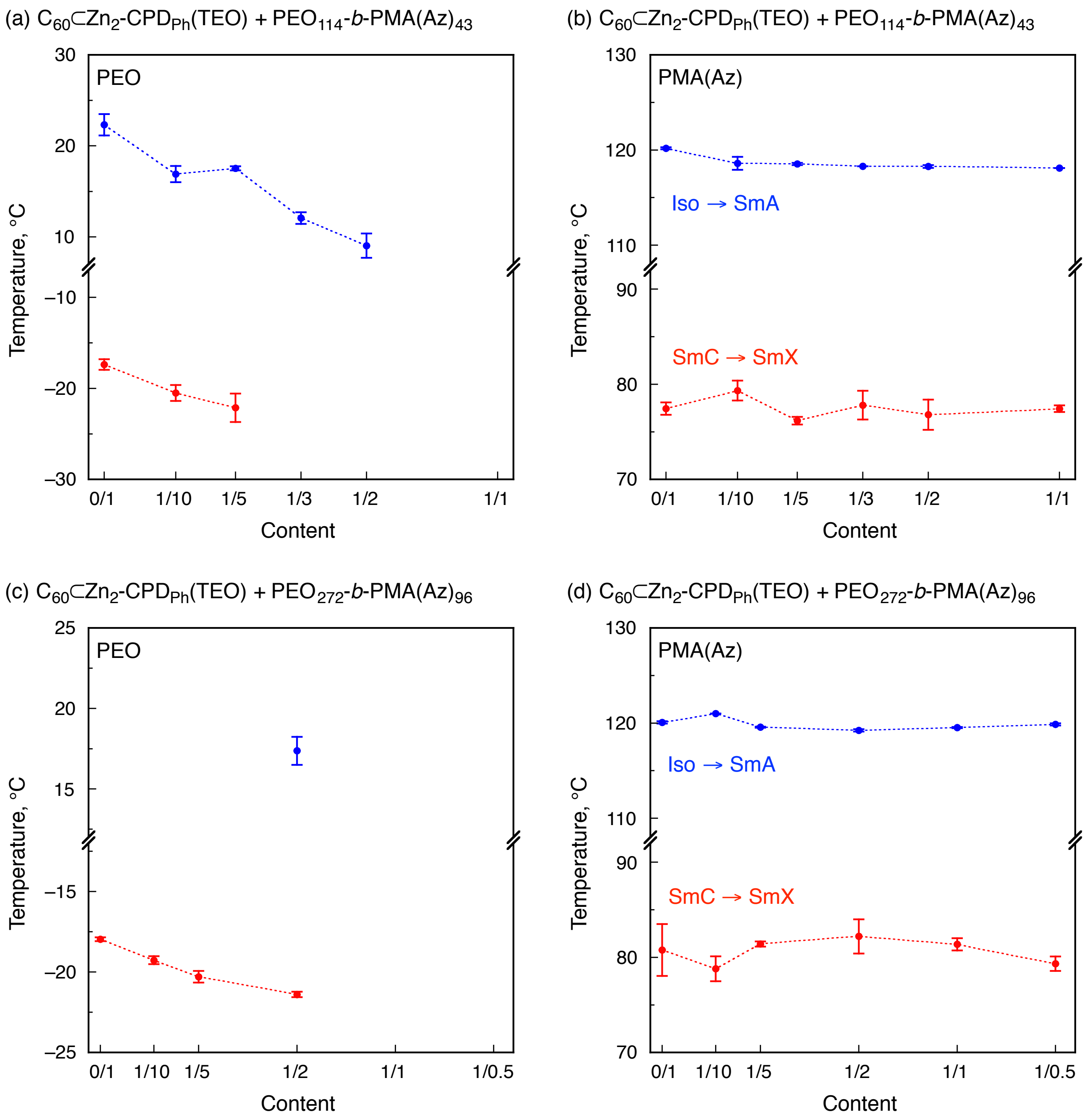

Figure S10. Transition temperature changes of (a,c) the freezing transitions of the PEO domains and (b,d) the Iso → SmA and the SmC → SmX transitions of the PMA(Az) matrix on the 1st cooling process in the course of mixing of C_{60}⊂Zn_2-CPD_{Ph}(TEO) into PEO_m-*b*-$PMA(Az)_n$. The ranges of the contents were (a,b) 0/1 ~ 1/1 and (c,d) 0/1 ~ 1/0.5. The lacks of data points are due to the absence of clear transition peaks. The temperatures and the standard deviations were calculated from three measurements for every sample.

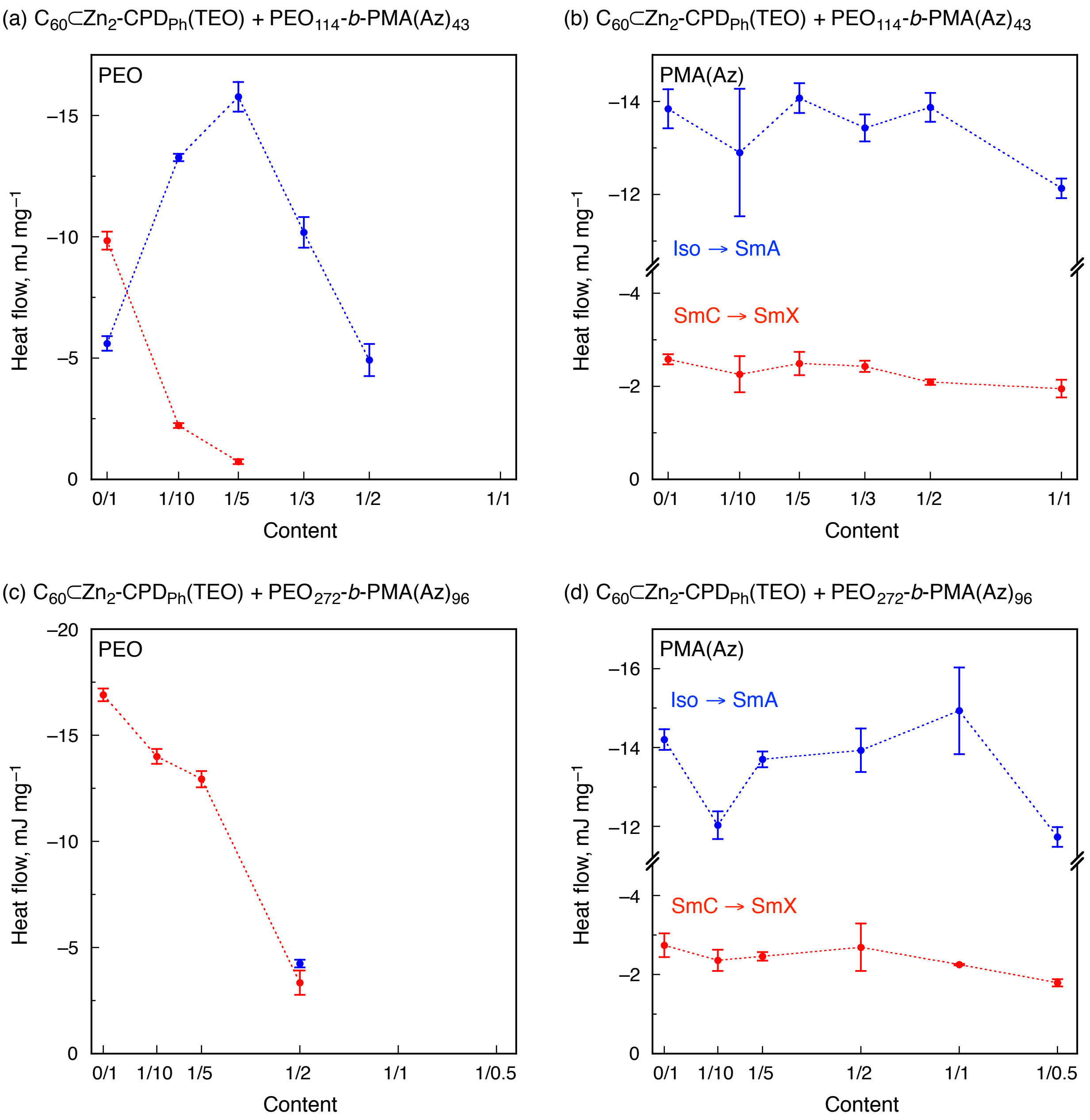

Figure S11. Transition temperature changes of (a,c) the freezing transitions of the PEO domains and (b,d) the Iso → SmA and the SmC → SmX transitions of the PMA(Az) matrix on the 1st cooling process in the course of mixing of $C_{60}{\subset}Zn_2$-CPD$_{Ph}$(TEO) into PEO$_m$-*b*-PMA(Az)$_n$. The ranges of the contents were (a,b) 0/1 ~ 1/1 and (c,d) 0/1 ~ 1/0.5. The lacks of data points are due to the absence of clear transition peaks. The enthalpies and the standard deviations were calculated from three measurements for every sample.

3.5. NMR spectroscopy.

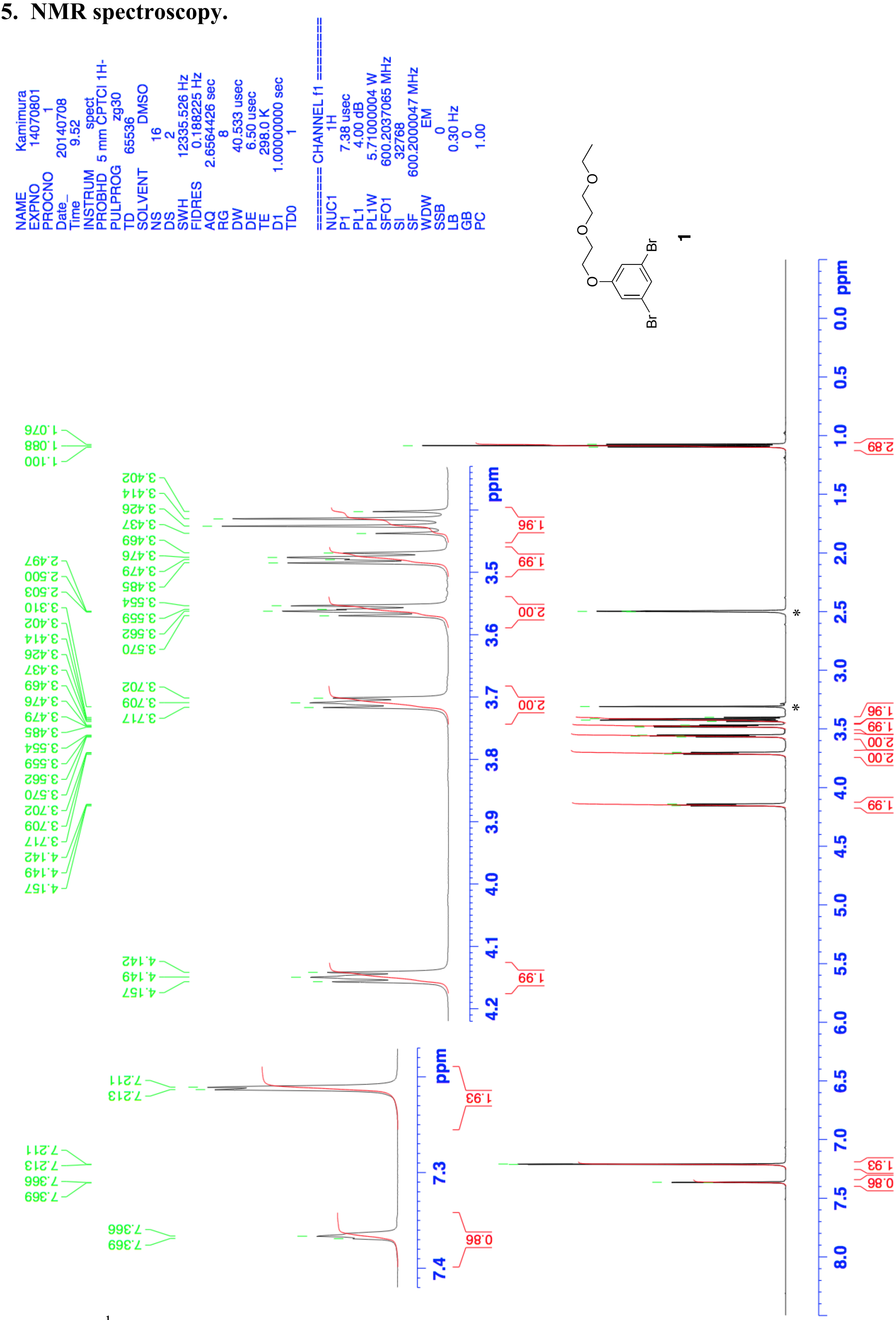

Figure S12. ^{1}H NMR spectrum of **1** in DMSO-d_6 at 25 °C.

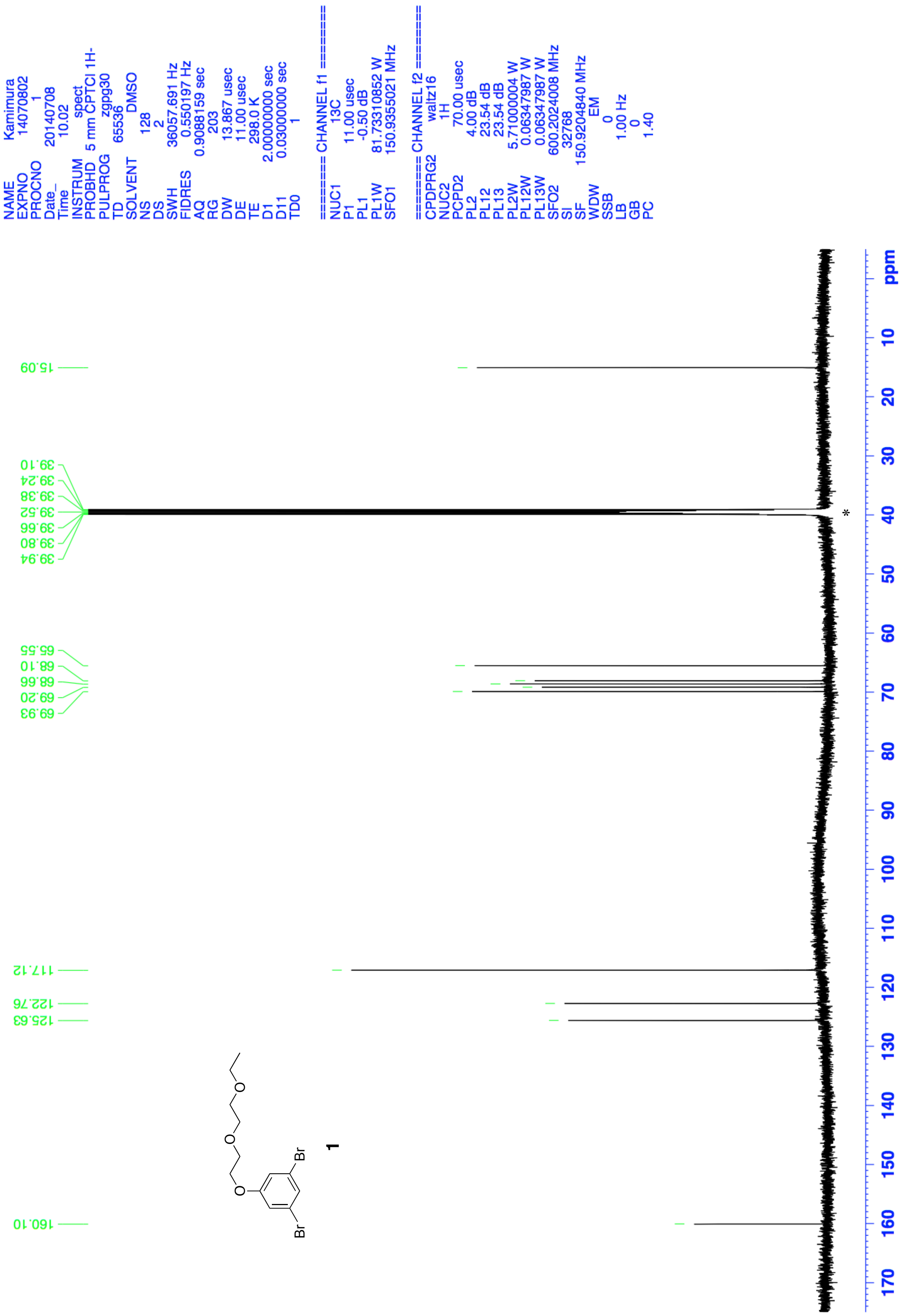

```
NAME          Kamimura
EXPNO         14070802
PROCNO               1
Date_         20140708
Time             10.02
INSTRUM          spect
PROBHD   5 mm CPTCI 1H-
PULPROG         zgpg30
TD               65536
SOLVENT           DMSO
NS                 128
DS                   2
SWH        36057.691 Hz
FIDRES      0.550197 Hz
AQ         0.9088159 sec
RG                 203
DW            13.867 usec
DE             11.00 usec
TE             298.0 K
D1        2.00000000 sec
D11       0.03000000 sec
TD0                  1

======== CHANNEL f1 ========
NUC1               13C
P1             11.00 usec
PL1            -0.50 dB
PL1W       81.73310852 W
SFO1      150.9355021 MHz

======== CHANNEL f2 ========
CPDPRG2        waltz16
NUC2                1H
PCPD2          70.00 usec
PL2             4.00 dB
PL12           23.54 dB
PL13           23.54 dB
PL2W        5.71000004 W
PL12W       0.06347987 W
PL13W       0.06347987 W
SFO2      600.2024008 MHz
SI               32768
SF        150.9204840 MHz
WDW                 EM
SSB                  0
LB                1.00 Hz
GB                   0
PC                1.40
```

Figure S13. ^{13}C NMR spectrum of **1** in DMSO-d_6 at 25 °C.

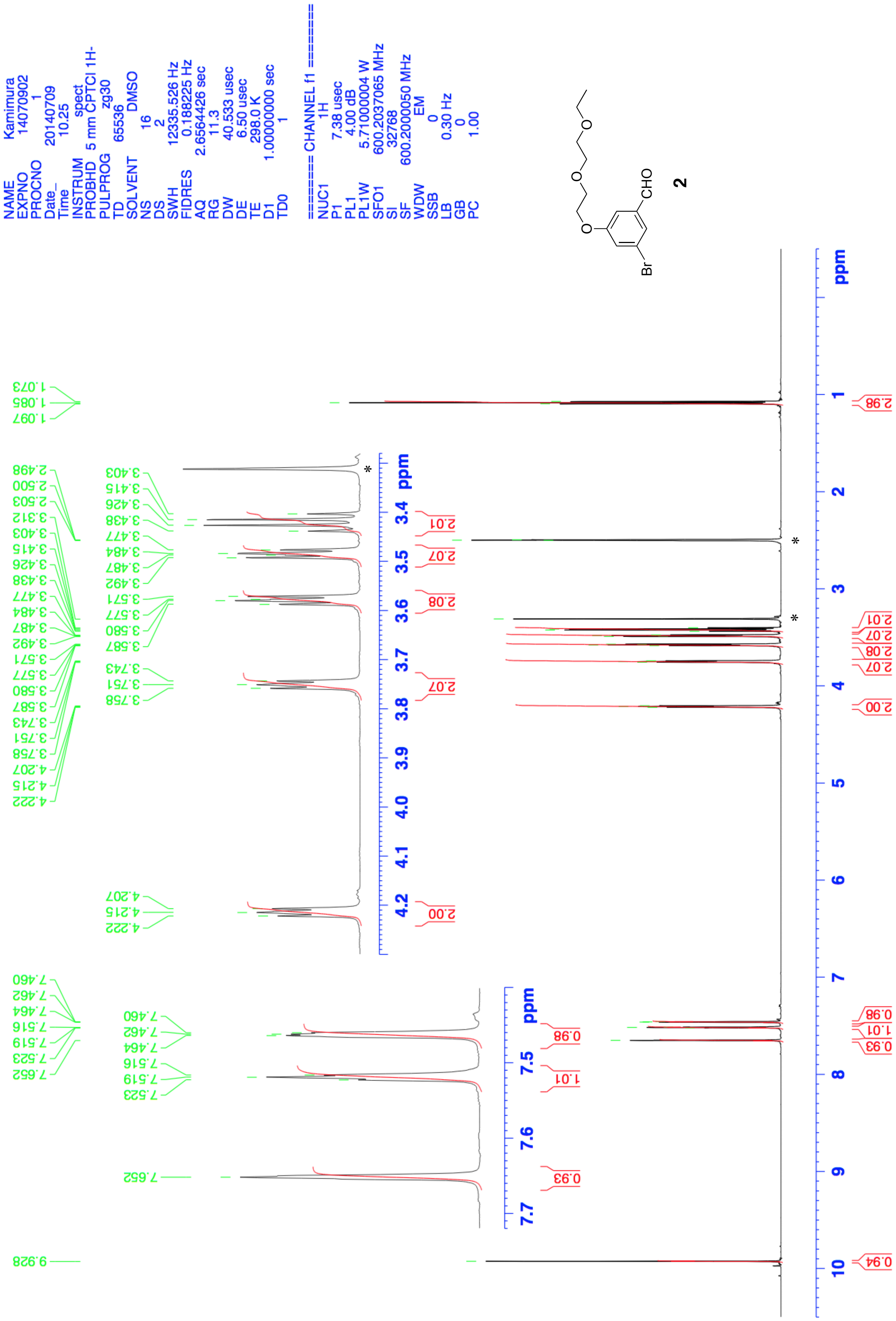

Figure S14. ^{1}H NMR spectrum of **2** in DMSO-d_6 at 25 °C.

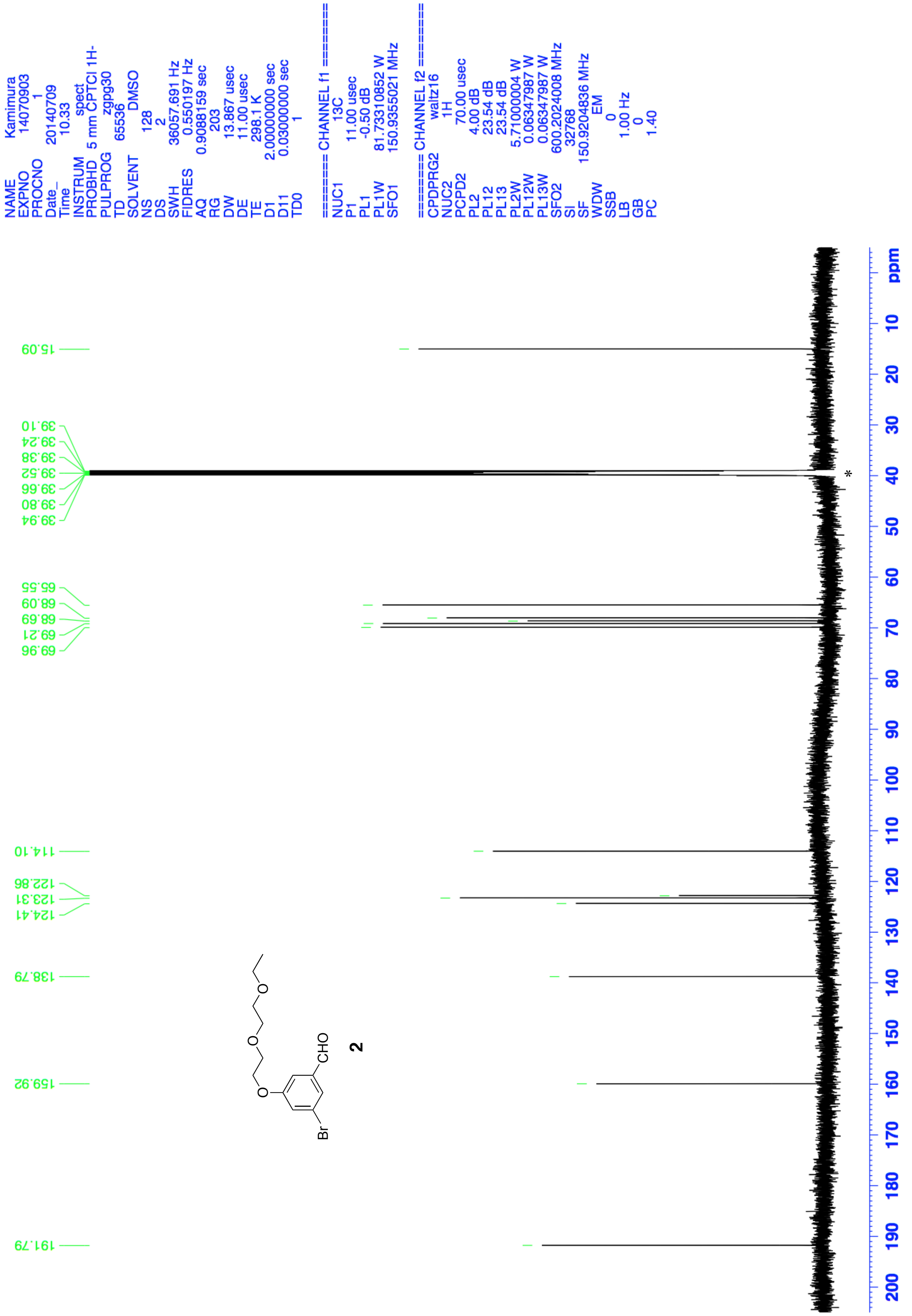

Figure S15. ^{13}C NMR spectrum of **2** in DMSO-d_6 at 25 °C.

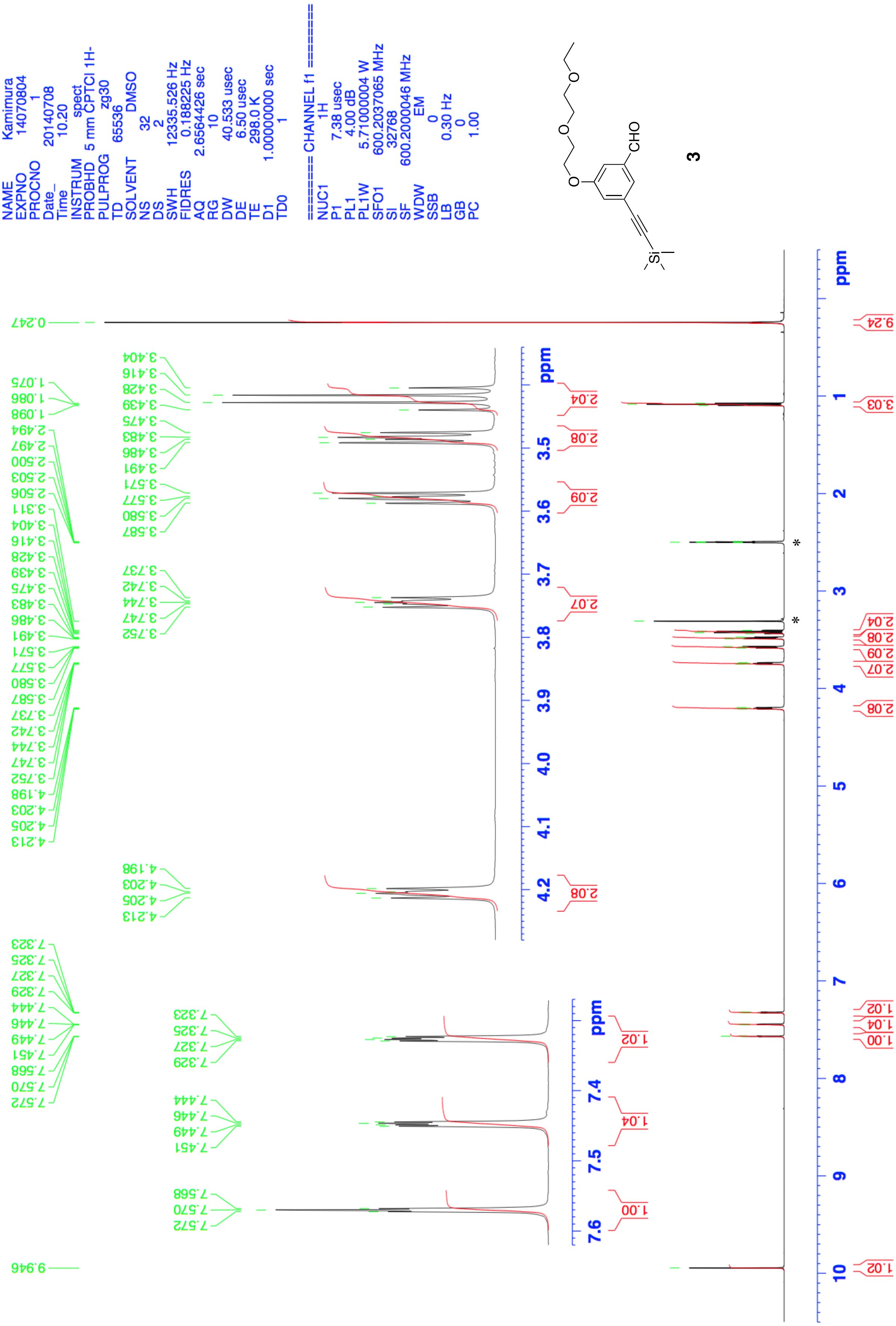

Figure S16. ^{1}H NMR spectrum of **3** in DMSO-d_6 at 25 °C.

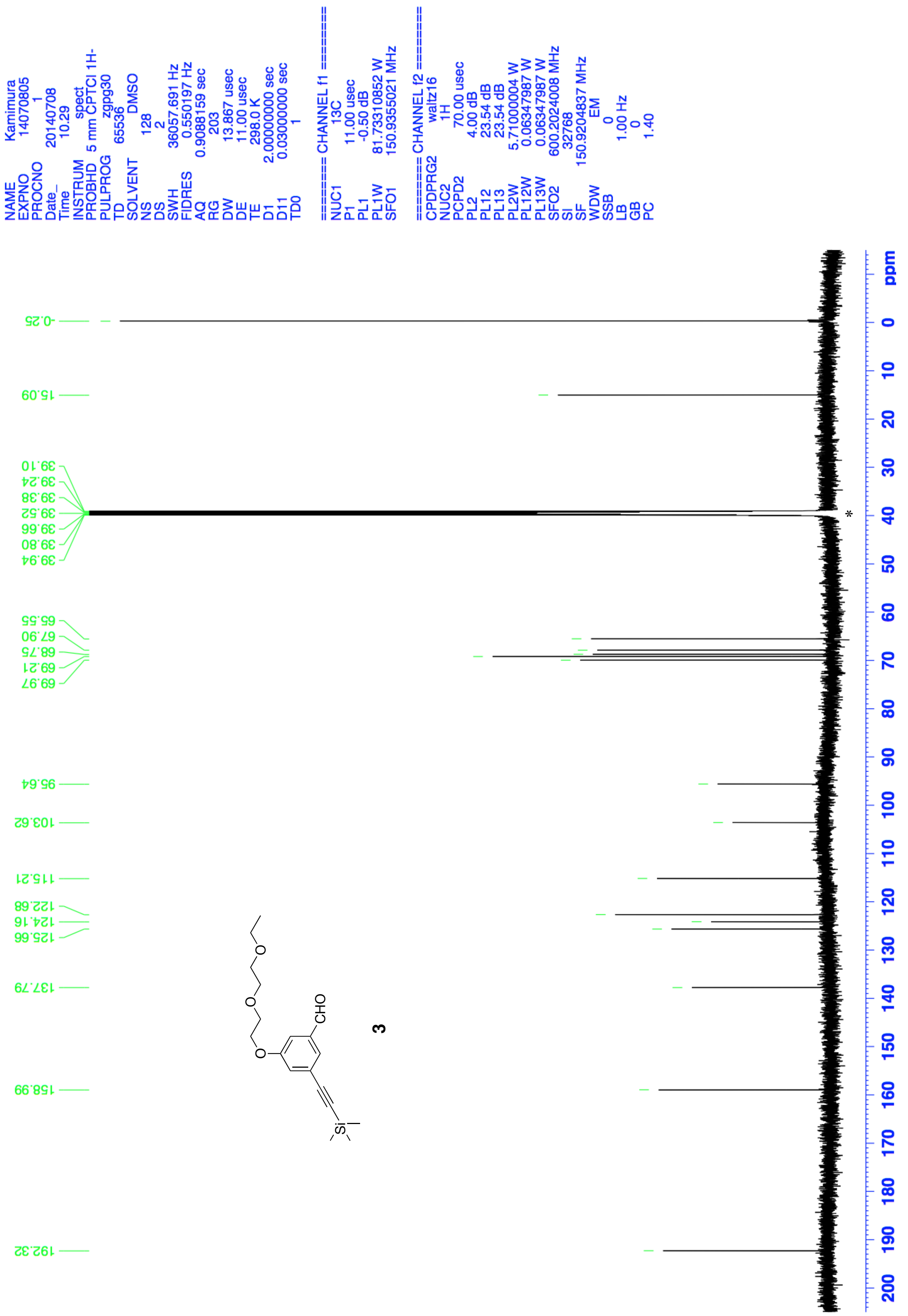

```
NAME       Kamimura
EXPNO      14070805
PROCNO            1
Date_      20140708
Time          10.29
INSTRUM       spect
PROBHD   5 mm CPTCI 1H-
PULPROG      zgpg30
TD            65536
SOLVENT        DMSO
NS              128
DS                2
SWH      36057.691 Hz
FIDRES    0.550197 Hz
AQ       0.9088159 sec
RG              203
DW           13.867 usec
DE            11.00 usec
TE            298.0 K
D1       2.00000000 sec
D11      0.03000000 sec
TD0               1

======== CHANNEL f1 ========
NUC1            13C
P1            11.00 usec
PL1           -0.50 dB
PL1W    81.73310852 W
SFO1    150.9355021 MHz

======== CHANNEL f2 ========
CPDPRG2     waltz16
NUC2             1H
PCPD2         70.00 usec
PL2            4.00 dB
PL12          23.54 dB
PL13          23.54 dB
PL2W     5.71000004 W
PL12W    0.06347987 W
PL13W    0.06347987 W
SFO2    600.2024008 MHz
SI            32768
SF      150.9204837 MHz
WDW              EM
SSB               0
LB             1.00 Hz
GB                0
PC             1.40
```

Figure S17. ^{13}C NMR spectrum of **3** in DMSO-d_6 at 25 °C.

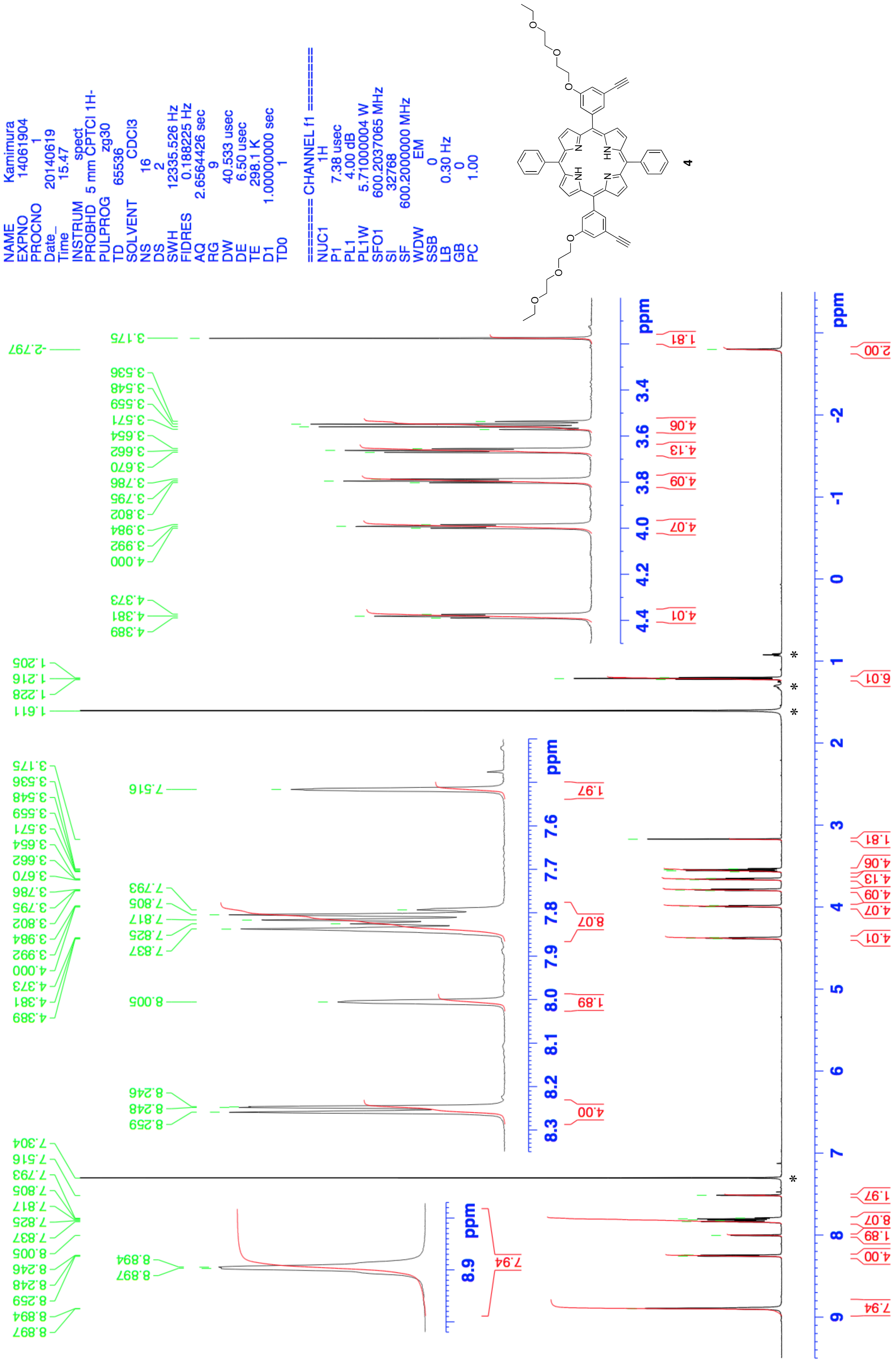

Figure S18. ^{1}H NMR spectrum of **4** in $CDCl_3$ at 25 °C.

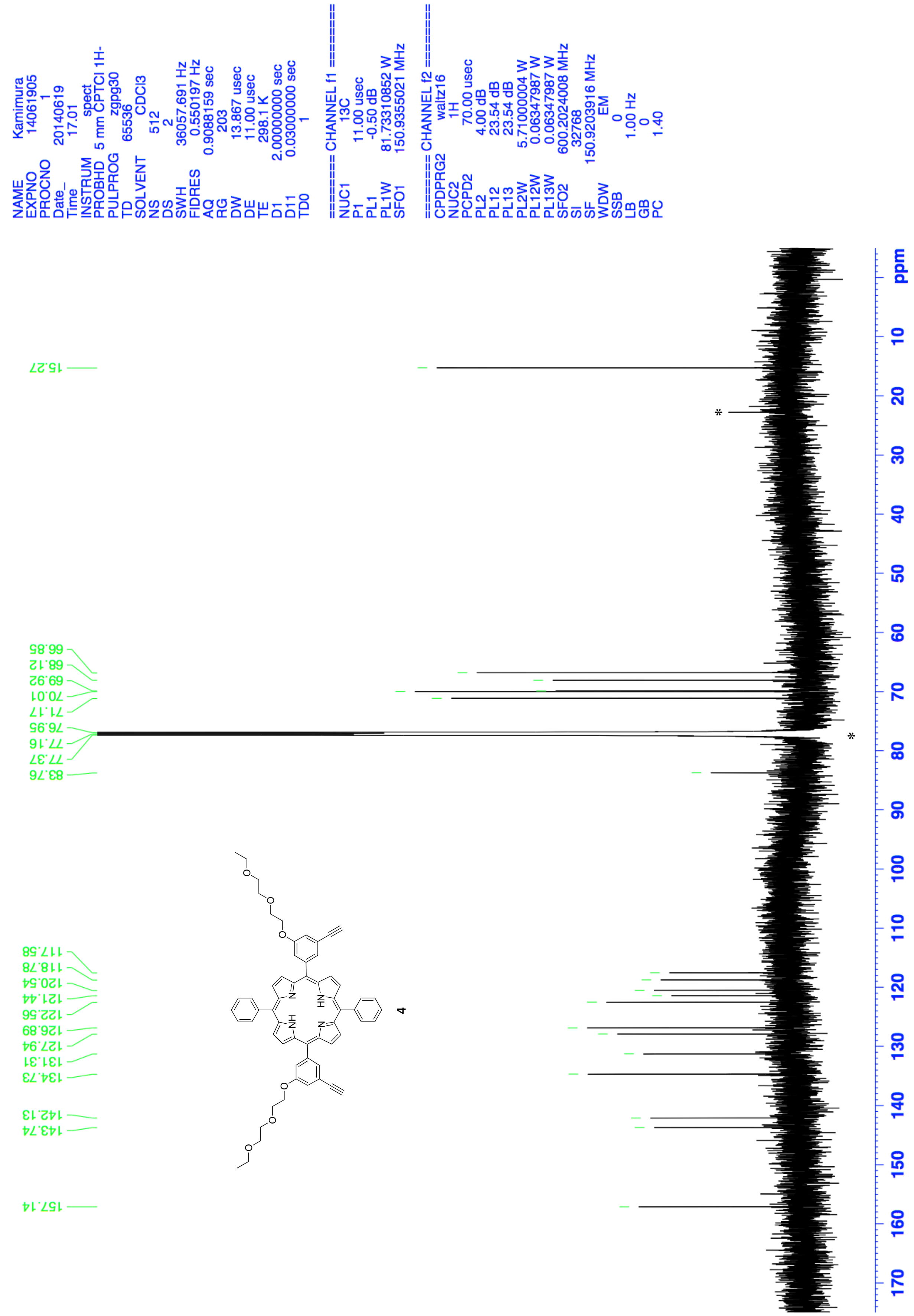

Figure S19. ^{13}C NMR spectrum of **4** in CDCl$_3$ at 25 °C.

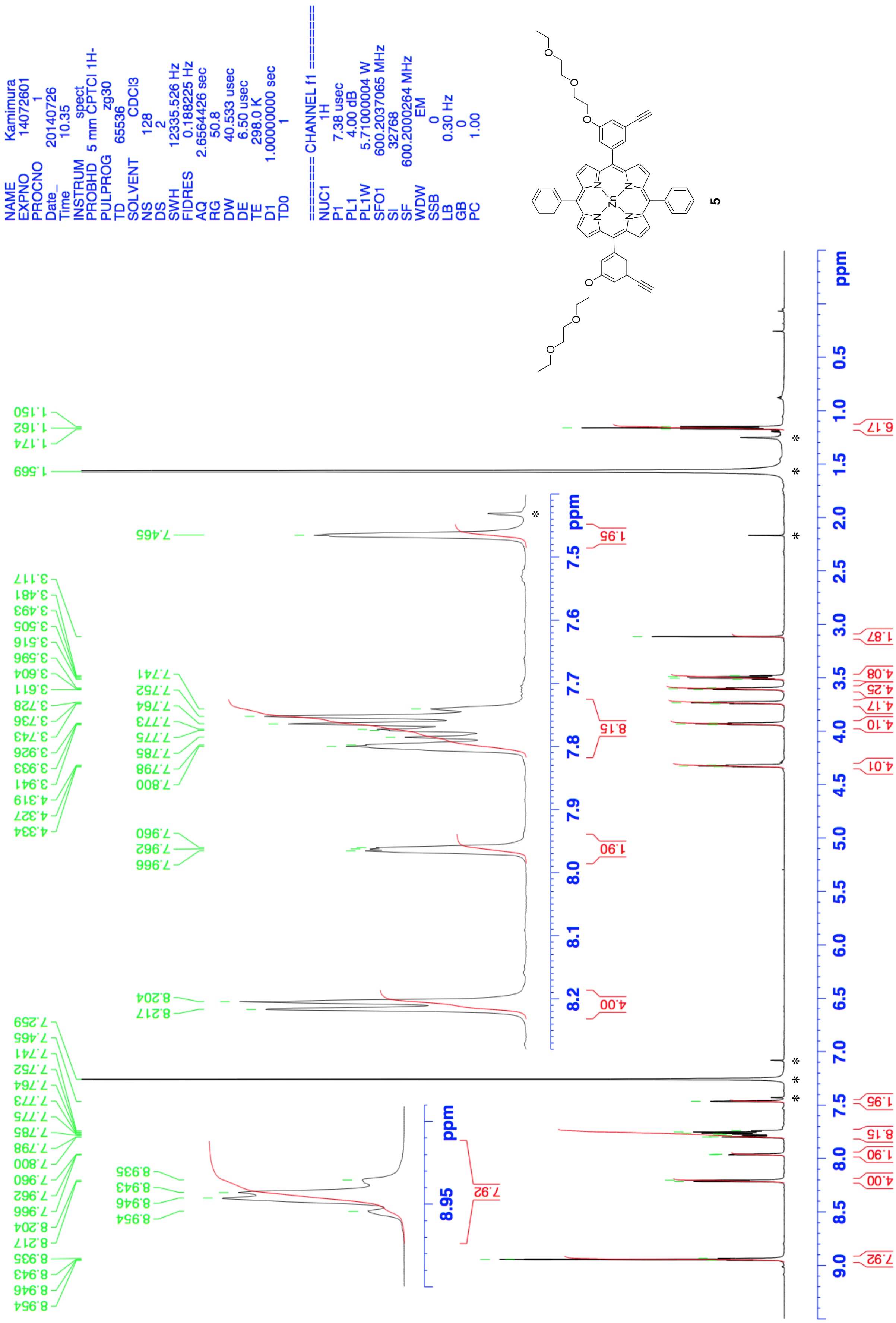

```
NAME            Kamimura
EXPNO           14072601
PROCNO                 1
Date_           20140726
Time               10.35
INSTRUM            spect
PROBHD    5 mm CPTCI 1H-
PULPROG             zg30
TD                 65536
SOLVENT            CDCl3
NS                   128
DS                     2
SWH         12335.526 Hz
FIDRES       0.188225 Hz
AQ         2.6564426 sec
RG                  50.8
DW           40.533 usec
DE             6.50 usec
TE               298.0 K
D1        1.00000000 sec
TD0                    1

======== CHANNEL f1 ========
NUC1                  1H
P1             7.38 usec
PL1              4.00 dB
PL1W       5.71000004 W
SFO1     600.2037065 MHz
SI                 32768
SF       600.2000264 MHz
WDW                   EM
SSB                    0
LB               0.30 Hz
GB                     0
PC                  1.00
```

Figure S20. ^{1}H NMR spectrum of **5** in $CDCl_3$ at 25 °C.

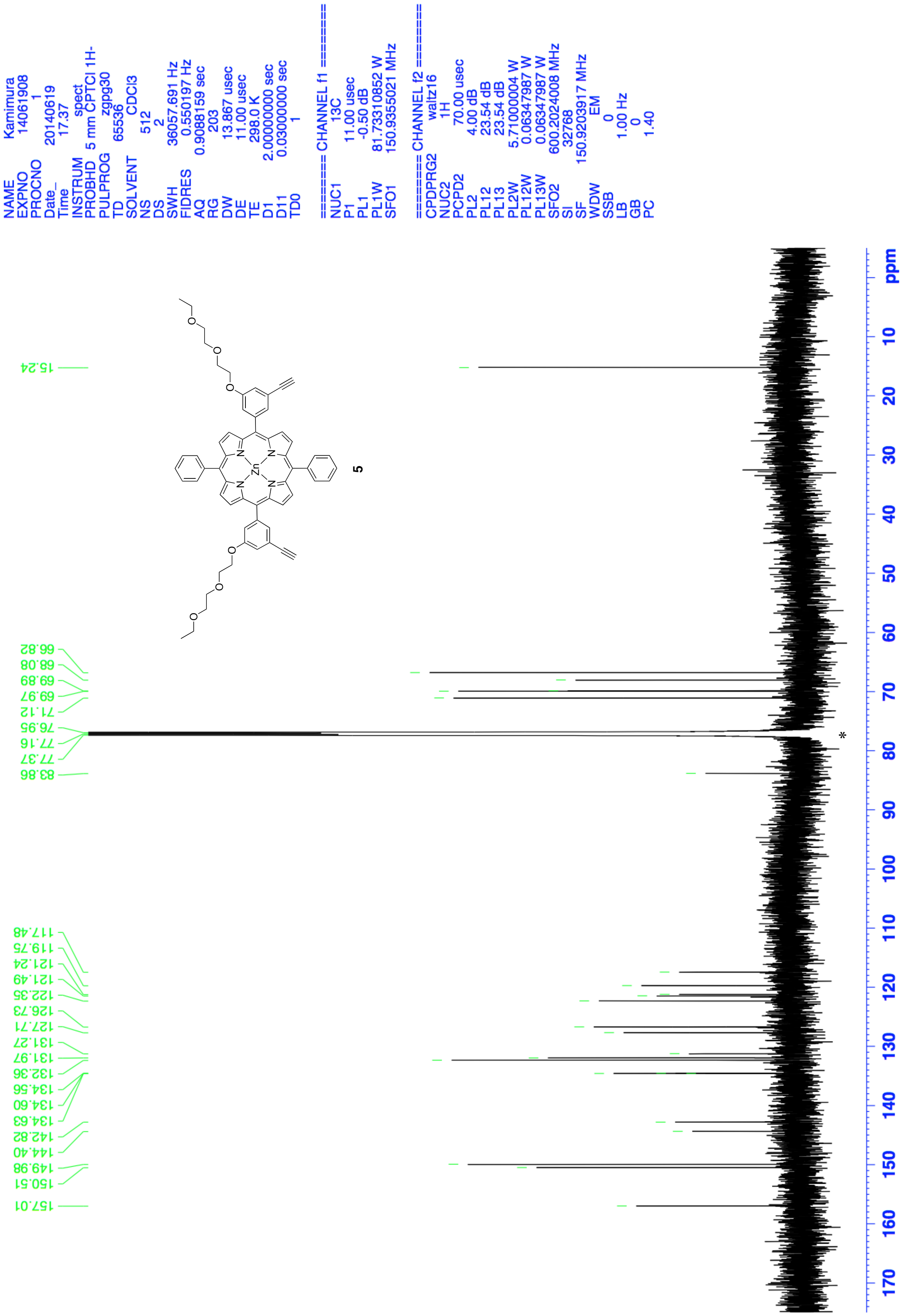

Figure S21. ^{13}C NMR spectrum of **5** in $CDCl_3$ at 25 °C.

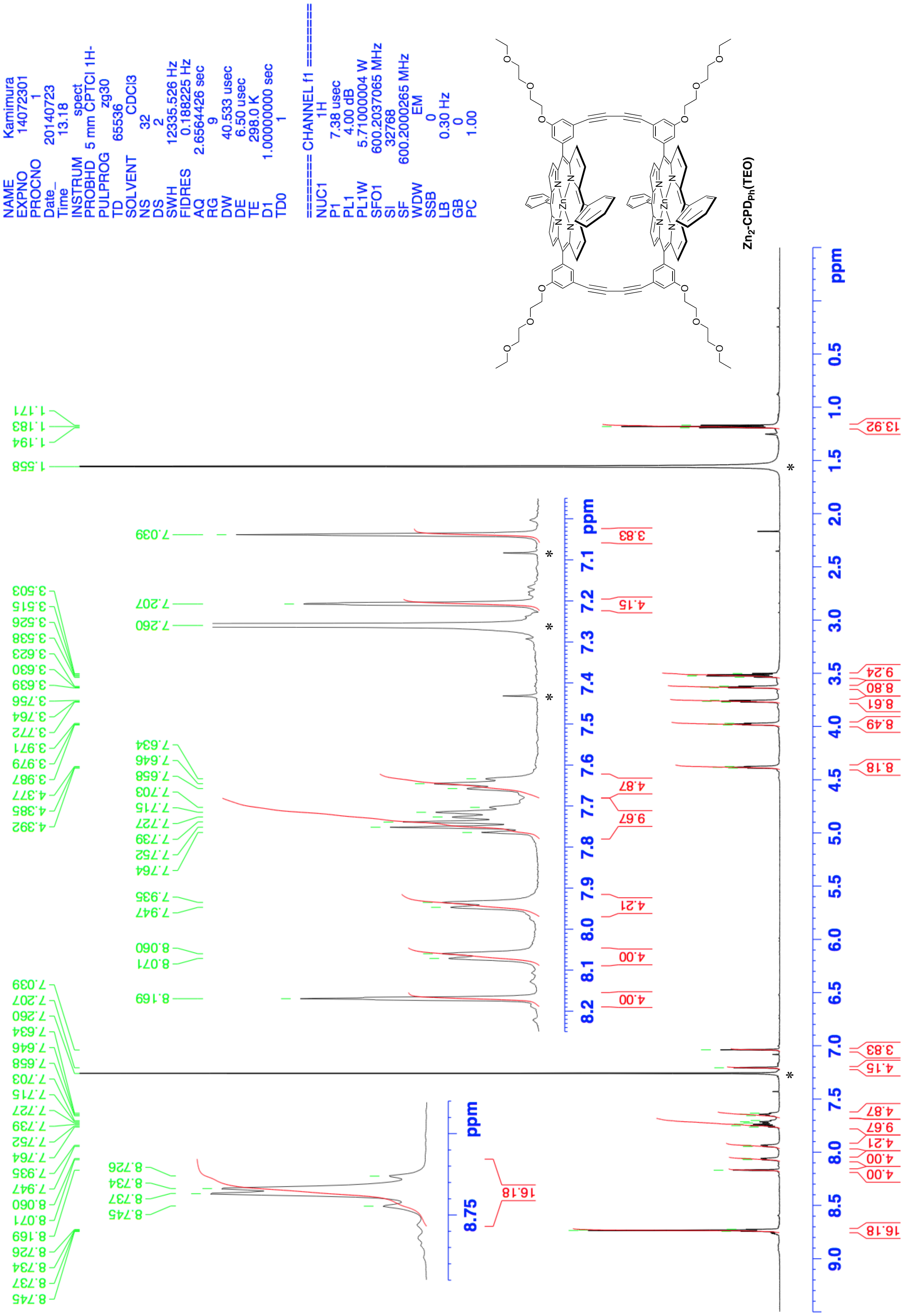

Figure S22. ^{1}H NMR spectrum of **Zn_2-CPD$_{Ph}$(TEO)** in $CDCl_3$ at 25 °C.

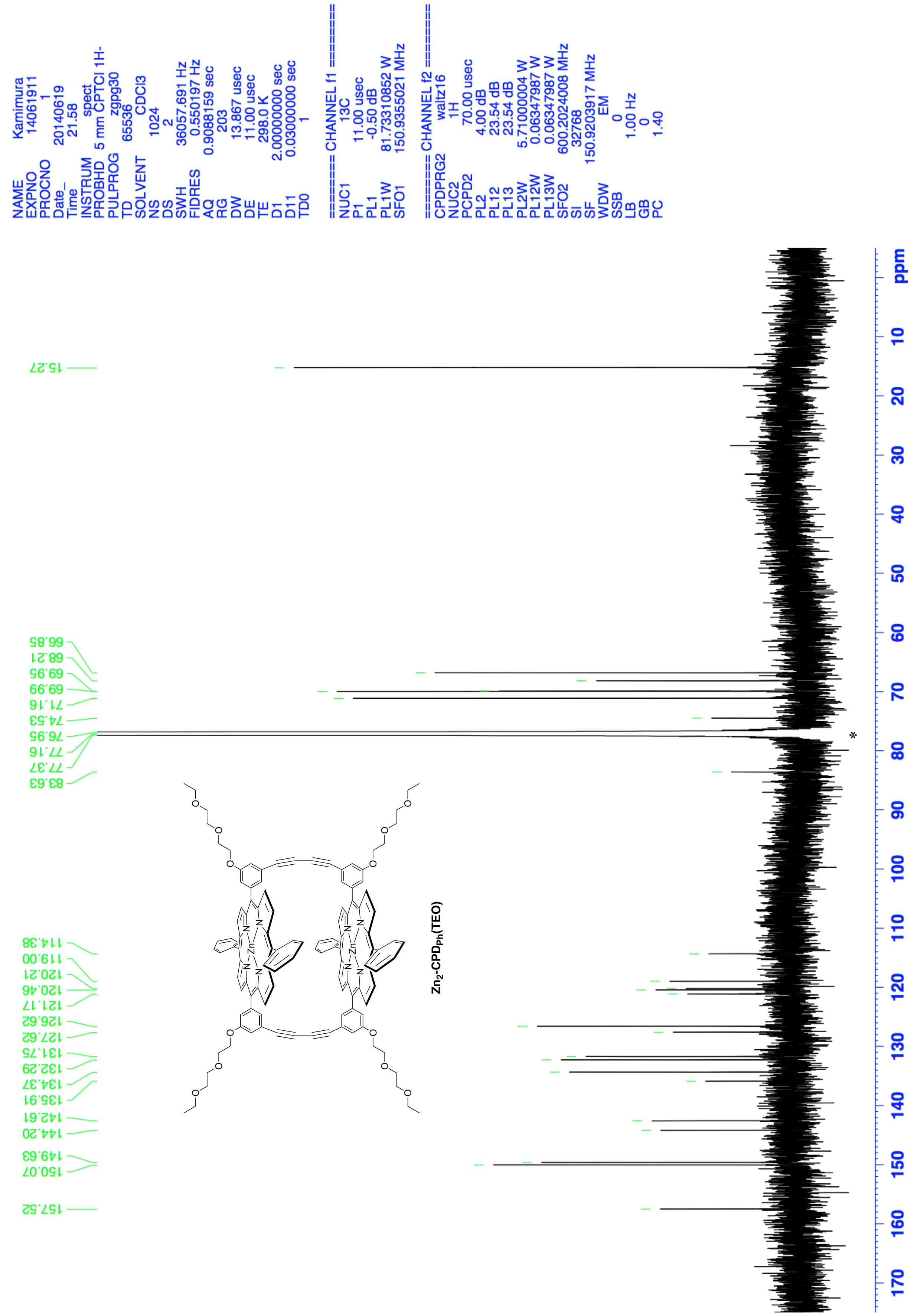

Figure S23. ^{13}C NMR spectrum of **Zn$_2$-CPD$_{Ph}$(TEO)** in CDCl$_3$ at 25 °C.

4. References

S1. M. Komura, K. Watanabe, T. Iyoda, T. Yamada, H. Yoshida and Y. Iwasaki, *Chem. Lett.*, 2009, **38**, 408–409.

S2. Y. Tian, K. Watanabe, X. Kong, J. Abe and T. Iyoda, *Macromolecules*, 2002, **35**, 3739−3747.

S3. Y. Zhang, C. Zhao, J. Yang, M. Kapiamba, O. Haze, L. J. Rothberg and M.-K. Ng, *J. Org. Chem.*, 2006, **71**, 9475–9483.

S4. I.-H. Kim, H.-J. Tsai, K. Nishi, T. Kasagami, C. Morisseau and B. D. Hammock, *J. Med. Chem.*, 2007, **50**, 5217–5226.

S5. T. Rohand, E. Dolusic, T. H. Ngo, W. Maes and W. Dehaen, *Arkivoc*, 2007, 307–324.

S6. The yield of the free-base porphyrin monomer **4** is relatively low in comparison with typical tetraphenylporphyrins (~30%). Although the reaction conditions have not been thoroughly optimized, possible reasons are the scrambling of the *meso*-substituents and the good solubility of **4** in MeOH at the recrystallization.